Anyons: A Pathway to Fault Tolerant Topological Quantum Computing

Author: Anirudha Bansal

Supervisor: Andrew Tolley

June 2023

Abstract

As classical machines reach a limiting factor of size and computing power, it becomes imperative that we research and develop the future of computation which is robust, powerful and can withstand the needs of modern civilisation. Since its initial proposal in 1988, quantum computing has been the perceived solution to this quandary. This literature review explores the theoretical framework required to build a fault-tolerant quantum computer through the use of non-Abelian anyons - quasiparticles found in fractional quantum Hall states and formed through vortices at specific Landau filling fractions. The topological properties of these quasiparticles allow the production of qubits that are tolerant to any local perturbations - creating a robust quantum computer than can perform exponential algorithms in polynomial time.

Contents

1 Introduction

The original definition of a computer "one who calculates, a reckoner, one whose occupation is to make arithmetical calculations" [1], swiftly changed with the realisation of Turing machines - such as the ENIAC. Computers became "electronic device used for storing and processing data, making calculations and storing machinery" [2]. ENIAC, the first programmable computer, weighed over 30 tonnes and required 200kW to run almost 20,000 vacuum tubes, hundreds of thousands of resistors and 1500 relays; could add, subtract, and store 10 digit numbers. [3] Over 70 years later, technology seems to be infinitely more advanced, with smartwatches capable of sending and receiving data through WiFi and Bluetooth, as well as measuring health data such as EKG and heart rate. Information can be stored in fingernail-sized microSD cards with terabytes of memory.

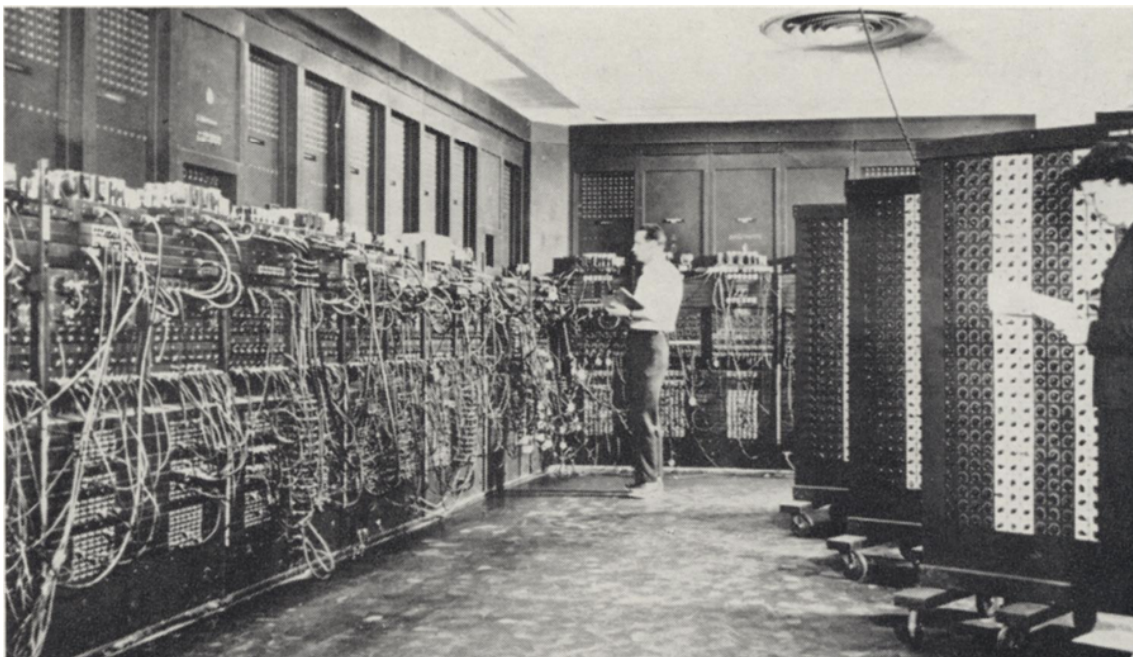Figure 1: The ENIAC's components took up the entire room in which it was located. Constant maintenance was required to ensure to running of the machine. [3]

However, as technology gets smaller, and more advanced, the electrical components, namely transistors, used to build gates are reaching a limiting factor. They work by controlling the flow of electrons through a circuit. If they become too small, electrons

start to exhibit quantum behaviour and can potentially tunnel their way through the gate - rendering the transistor useless. As we reach this impasse, it becomes vital to find a solution as civilisation becomes increasingly dependant on computers.

A potential solution to this problem is quantum computation, an answer that was theorised in the 1980s, and has taken many forms since. A quantum system that can represent a two state superposition is known as a qubit and is integral to the method used in making a quantum computer powerful. Using this idea, quantum information theorists have spent decades coming up with a variety of different algorithms which illustrate how powerful a quantum computer is. The Deutsch-Jozsa algorithm developed in 1992 demonstrates how a problem solved in exponential time using a classical computer can be solved by a quantum algorithm in polynomial time. [4]
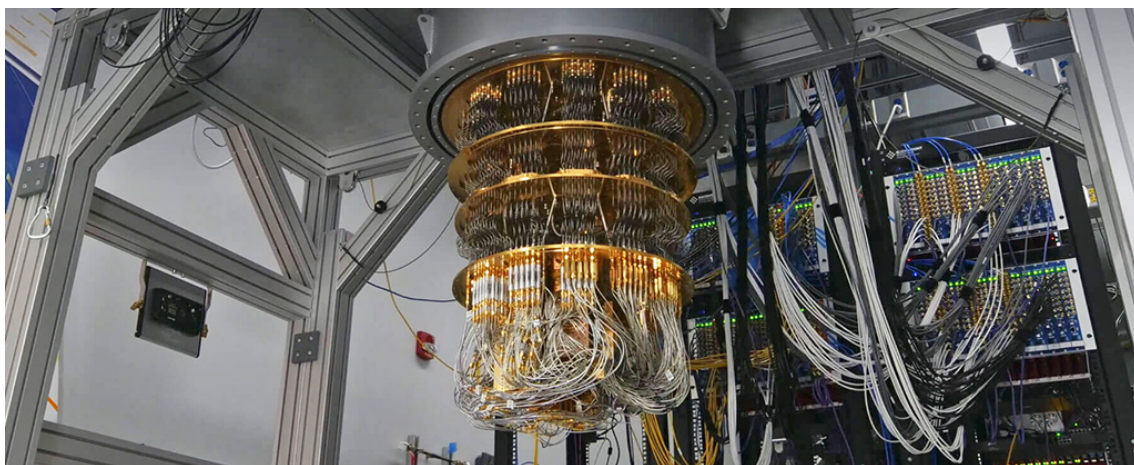
Figure 2: One of the quantum computers used by Google (Google Quantum AI). [5]

Shor's algorithm is another example of this phenomenon where a quantum algorithm can easily prime factorise large numbers in polynomial time [6]. Since most encryption algorithms use the fact that classical computers take an exponential order of time to prime factorise, a current topic of research for many companies is quantum encryption. Despite these algorithms being built specifically for quantum computers, research is also conducted to ensure that the results of these algorithms are indeed unique to quantum computers and cannot be mimicked using the classical kind. In March 2023, a paper was published proving that, unlike these algorithms, Grover's algorithm can be expressed

classically.[7]

However, there is one great problem scientists face when building a quantum computer - decoherence. The macroscopic world at high temperatures contain a lot of interacting particles that create a lot of quantum noise. Quantum noise are local perturbations to the wavefunction caused by environmental factors such as temperature, spontaneous emission due to vacuum energy and measurement errors due to the Heisenberg uncertainty principle. Most theorised and implemented methods of quantum computing use qubits which require a very unstable state of quantum coherence - e.g. entangled electron spins [8], optical modes of photons [9] or energy levels of an ion [10]. This requires the qubits to be kept in a low temperature, noise free system which is not compatible with the macroscopic world.

One solution to this is topological quantum computing (TQC). This paper aims to delve into the specifics behind how the properties of quantum mechanics in two dimensions can provide the platform to build a fault tolerant quantum computer. Instead of creating a local state to encode information as described above, a TQC utilises the global properties of a 2D topology, making it tolerant against local quantum perturbations.

In section **??**, a type of exotic particle, non-Abelian anyons will be introduced. Fibonacci anyons, the simplest non-Abelian anyon, are braided around each other to implement quantum computations. All computations done using this method depend entirely on the topology of the braiding, meaning any local perturbation doesn't affect the system.

This paper will provide a thorough explanation of how topology affects the quantum properties encoded in the wavefunction of a particle. We will explore how two dimensional topology gives rise to a new type of particles, coined "anyons" by Frank Wilczek in 1982, and how Fibonacci anyons, whose world lines can be represented mathematically by knot theory, allow the topology to represent a quantum computer. The paper will explain what gives rise to errors and explore the specifics of why TQCs are unaffected by those phenomena.

2 Background Information

2.1 Particles in 3D

The Standard Model describes particles in three dimensions. They are represented by the group $SU(3) \times SU(2) \times U(1)$. They describe the fundamental particles that make up the universe, namely, leptons, quarks, gauge bosons and the Higgs boson. These particles are split into two groups due to the different statistics they obey. The first group, bosons, have integer spins and obey Bose-Einstein statistics. The other group, fermions, have half integer spins and obey Fermi-Dirac statistics. Sections 2.1.1 and 2.1.2 will describe these statistics in detail.

2.1.1 Bosons

Satyendra Nath Bose, an Indian mathematician, was the instrumental force behind quantum statistics and his contribution came at a pivotal turning point between the old quantum theories postulated by scientists like Albert Einstein and Neils Bohr, and the rapidly developing quantum mechanics introduced by Heisenberg, Schrodinger and Dirac. While lecturing at the university of Dhaka, S. N. Bose was attempting to demonstrate the ultraviolet catastrophe when using a classical theory to show the results of blackbody radiation. During his calculations, he made a statistical error, implying that a fair coin would have a bias, such that the probability of two heads would be $\frac{3}{4}$. This 'error' resulted in the measured blackbody radiation - without an ultraviolet catastrophe. S. N. Bose wondered if maybe this wasn't an error and, following this theory, he formed what would become the basis of Bose-Einstein statistics.

In 1924, Satyendra Nath Bose attempted to publish his theory "Planck's Law and the light quantum hypothesis", though this was met with resistance within the scientific community and not accepted - the reason for this is unknown. To get the paper published, S. N. Bose sent his paper to Albert Einstein for his consideration and requested that the paper be translated to German and be published in the *Zeitschrift für Physik* [11].

Einstein immediately recognised the potential of this theory and had it published, along with his own supporting paper where he generalised the theory from photons to atoms.

Bose-Einstein statistics describe elementary particles called bosons, whose key feature is that the particles are indistinguishable; i.e. the wavefunction is invariant under exchange of identical particles. Bose represented photons as quanta of radiation in a volume V and energy $E = h\nu_s$ where s is an integer. By subdividing the momentum phase space into cells of magnitude h^3, Bose showed that

$$E = \sum_s \frac{8\pi h\nu^{s^3}}{c^3} \frac{V}{e^{\frac{h\nu^s}{kT}} - 1},$$ (1)

which is equivalent to Planck's formula, however he achieved this without using the classical assumptions - unlike all papers that had predated his. [12][13]. The expectation value for the number of particles in an energy state i is then given by

$$\overline{n}_i = \frac{g_i}{e^{(\epsilon_i - \mu)/k_B T} - 1},$$ (2)

where n_i is the expectation value of the number of particles in state i with energy level ϵ_i and degeneracy g_i, μ is the chemical potential (energy released or absorbed due to change in particle number), k_B is the Boltzmann constant, and T is the temperature of the system. At higher temperatures, low particle density state, where $e^{(\epsilon_i - \mu)/k_B T} \gg 1$, the system resembles the classical Maxwell-Boltzmann distribution

$$\overline{n}_i = \frac{g_i}{e^{(\epsilon_i - \mu)/k_B T}}.$$ (3)

Bosons are indistinguishable particles which are defined to be symmetric under exchange. In a relativistic theory, the spin-statistics theorem dictates that bosons must have integer spin. These particles can be elementary, e.g. photons and gluons, or can be made up of an array of particles with half integer spins summing to integer spins, e.g. mesons made of 2 quarks. Mathematically, bosons are described by gauge fields, or scalar

fields - both of which solve the Klein-Gordon equation.

Gauge bosons - with spin 1, are represented by vector fields with SU(3), SU(2) and U(1) symmetries to represent gluons, electroweak bosons and photons, respectively. The terms in the Standard Model Lagrangian which describes these particles are

$$\mathcal{L} = -\frac{1}{2}\text{Tr}G_{\mu\nu}G^{\mu\nu} - \frac{1}{2}\text{Tr}W_{\mu\nu}W^{\mu\nu} - \frac{1}{4}F_{\mu\nu}F^{\mu\nu}, \tag{4}$$

where $G_{\mu\nu}$, $W_{\mu\nu}$ and $F_{\mu\nu}$ are the field strength tensors for the SU(3), SU(2) and U(1) gauge bosons, respectively [14]. Explicitly, $F_{\mu\nu} = \partial_\mu A_\nu - \partial_\nu A_\mu$, $G_{\mu\nu} = \partial_\mu C_\nu - \partial_\nu C_\mu - ig_s[C_\mu, C_\nu]$, where g_s is the strong coupling and $W_{\mu\nu} = \partial_\mu B_\nu - \partial_\nu B_\mu - ig_w[B_\mu, B_\nu]$, where g_w is the weak coupling and A_μ, B_μ, C_μ are vector fields.

Scalar bosons, with spin 0, are described by scalar fields, and describe the Higgs boson in the Standard Model. The Lagrangian describing the Higgs boson is

$$\mathcal{L} = (D_\mu\phi)^\dagger D^\mu\phi + \mu^2\phi^\dagger\phi - \frac{1}{2}\lambda(\phi^\dagger\phi)^2, \tag{5}$$

where ϕ is an n-component scalar field, μ^2 is the mass term for the Higgs field, and λ is the Higgs self coupling [14]. It is important to note that these are relativistic fields which are useful to describe elementary particles. However, composite bosons (e.g. He-4) arise in many realistic applications and can be described by non-relativistic field theories similar in form to the above but with greater freedom in the allowed interactions.

2.1.2 Fermions

In 1926, Following the work on B-E statistics, Enrico Fermi [16] and Paul Dirac [15] independently formulated statistics for fermions - now known as Fermi-Dirac statistics.[15] [16] A fermionic state, described by such a statistical model, must obey the Pauli exclusion principle - two fermions in the same quantum system cannot occupy the same quantum state simultaneously. Fermions are defined as states in a Hilbert space that gain a negative sign under the exchange of two particles. In a relativistic theory, the spin-statistics

theorem imply that fermions are particles with half-integer spin. These particles can be elementary - such as quarks and leptons in the Standard Model - or be made of multiple particles summing to half integer spins - e.g. baryons.

Mathematically, spin $\frac{1}{2}$ fermions are described by four component Dirac spinors, solutions to the Dirac equation $(i\not{\partial} - m)\psi(x)$, where ψ is the Dirac spinor and $\not{\partial} = \gamma^\mu \partial_\mu$ - γ^μ are the gamma matrices of the Clifford algebra. Associated with these Dirac particles, there exists anti-particles, represented by a $\overline{\psi} \equiv \psi^\dagger \gamma^0$ such that $\overline{\psi}\psi$ is Lorentz invariant.

In 1937, Ettore Majorana noticed that a spin $\frac{1}{2}$ particle could be described by a wholly real wavefunction, and so $\overline{\psi} = \psi$ [17]. This wavefunction describes a neutral fermion that is it's own antiparticle - a Majorana fermion. Though there has been no experimental evidence of Majorana fermions, neutrinos in the Standard Model have been hypothesised to be potential candidates for such a particle. The Lagrangian for the early Standard Model includes terms describing the quarks and leptons, although the neutrino in the early theory is formulated to be massless. At present, there is discord within the scientific community as to how neutrinos gain their mass. A simple Lagrangian with massless neutrinos can be written as

$$
\begin{aligned}
\mathcal{L} = &\sum_{f=1}^{3} \left(\overline{\ell}_L^f i\not{D}\ell_L^f + \overline{\ell}_R^f i\not{D}\ell_R^f + \overline{q}_L^f i\not{D}q_L^f + \overline{d}_L^f i\not{D}d_L^f + \overline{u}_L^f i\not{D}u_L^f \right) \\
&- \sum_{f=1}^{3} y_\ell^f \left(\overline{\ell}_L^f \phi \ell_R^f + \overline{\ell}_R^f \phi^\dagger \ell_L^f \right) \\
&- \sum_{f,g=1}^{3} \left(y_d^{fg} \overline{q}_L^f \phi d_R^g + (y_d^{fg})^* \overline{d}_R^g \phi^\dagger q_L^f + y_u^{fg} \overline{q}_L^f \tilde{\phi} u_R^g + (y_u^{fg})^* \overline{u}_R^g \tilde{\phi}^\dagger q_L^f \right)
\end{aligned}
\tag{6}
$$

where the y_e^f terms are the Yukawa couplings, $\ell_{L/R}^f$ are leptons, up and down quarks are $u_{L/R}^f$ and $d_{L/R}^f$, respectively, and quarks are represented as $q_{L/R}^f = (u_{L/R}^f, d_{L/R}^f)^{\mathrm{T}}$. [14]

Fermi-Dirac statistics describes the distribution of identical fermions in a thermodynamic equilibrium, where the expectation value of fermions in a single particle state i

is

$$\overline{n}_i = \frac{1}{e^{(\epsilon_i - \mu)/k_B T} + 1},$$ (7)

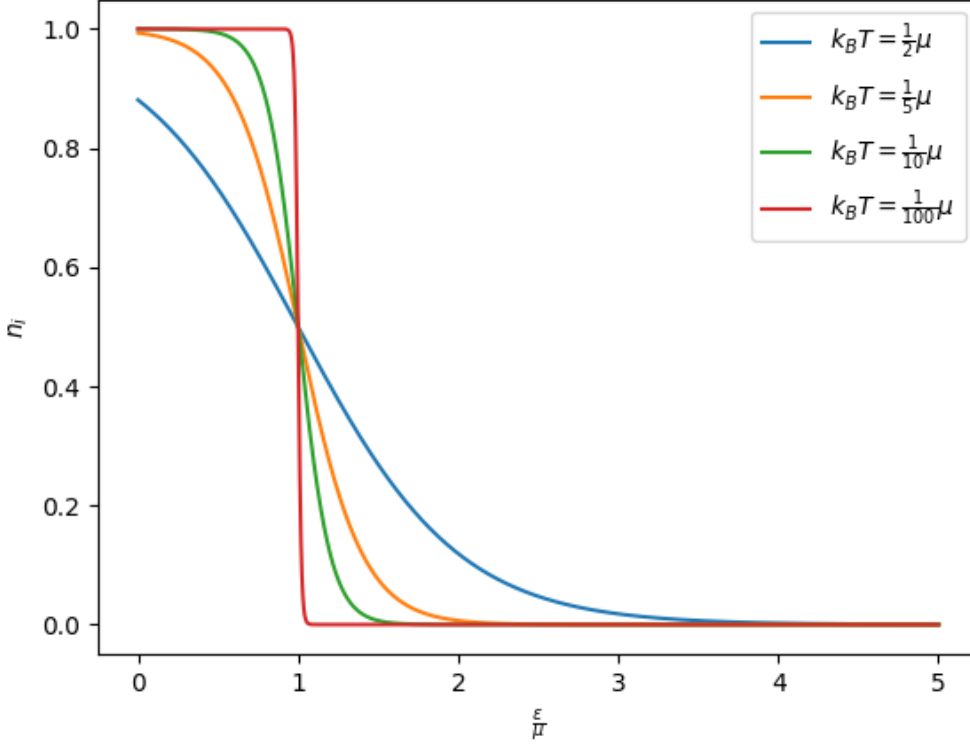with all the same definitions as Eqn. 2.

Figure 3: Graph illustrating the Fermi-Dirac distribution for different energy states. Different lines show different temperature scales and how that effects the distribution.

This distribution encapsulates the Pauli exclusion principle since $0 \leq \overline{n}_i \leq 1$, for any values of constants. The graph in Fog. 3 shows how the expectation value changes for different energies ϵ at different temperatures T, scaled in terms of the chemical potential μ. As can be seen, for all temperatures, when $\frac{\epsilon}{\mu} = 1$, the expectation value of fermions is exactly $\frac{1}{2}$ which is what one would expect when the energy is exactly the chemical potential. As with the Bose-Einstein distribution, in the low particle density limit and high temperature limit, one can see that $e^{(\epsilon_i - \mu)/k_B T} \gg 1$, therefore the Fermi-Dirac distribution approaches the classical Maxwell-Boltzmann distribution.

The formulation of Fermi-Dirac statistics had a vast impact on the understanding of

fermionic systems. Following the inception of the model, Arnold Sommerfeld, a German theoretical physicist, published the Drude-Sommerfeld model describing free electrons through a metal lattice of ions. This model successfully described relationships between electrical and thermal conductivity, as well as electron heat capacity (amongst others concepts) solving discrepancies that the previous Drude model had provided.

2.1.3 Quasiparticles

"Quasi" is a term used to describe something that almost is, but not completely - a statement that describes quasiparticles remarkably accuractely. While particles can exist in free space, and have independent properties such as mass, spin and charge, quasiparticles are quanta of energy which gain their intrinsic properties via the medium through which they are travelling. Therefore, quasiparticles can only exist within a medium and are often used as a method of simplifying problems in condensed matter physics. The theory was developed in 1941 by Lev Landau, who used this idea to look at the idea of superfluidity in Helium. [18]

2.2 Fractional Quantum Hall States

Due to the vast leaps made in material synthesis to satisfy the demands of increasingly powerful electronic device, extremely pure ultra-thin semiconductors are produced regularly. Such advancements have made it possible for scientists to create and study two dimensional electron systems - whether that is single particle, or many particles interacting with each other to form bizarre quantum effects: sections 2.2.2 and 2.2.3, respectively. However, before exploring these quantum phenomena, it is important to understand the classical electromagnetism which is behind the quantum behaviour we observe.

2.2.1 Hall Effect

In 1879, Edwin Hall was researching the effects of Maxwell's equations, specifically looking at the effects of a magnetic fields on the carriers of electric currents - later discovered

to be electrons. He found that upon applying a magnetic field to a conductor carrying current perpendicular to the field, a potential difference is produced transverse to both current and magnetic field - illustrated in Fig. 4. [19]

The diagram shows a potential difference V_x flowing across the plate with dimensions $l \times w \times h$ with a current I_x. The path of the electron (dark blue) is shown to be deflected by the magnetic field B_z, however, as electrons start to gather on the left hand side, the electric field E_y is produced, straightening out the path of electrons, shown by the dashed line. The Hall voltage created by this is $V_y = \frac{IB_z}{neh}$, where n is the electron density and e is the electron charge.
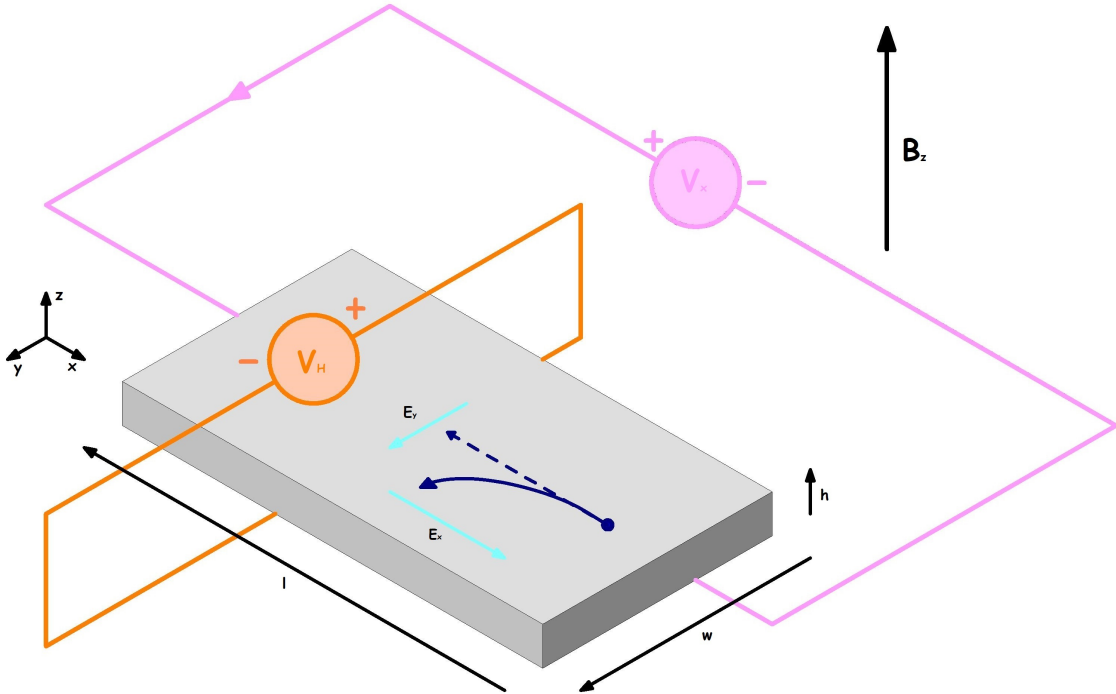

Figure 4: V_x voltage is sent through the plate with a current I while a magnetic field B is sent through it. Contacts are placed on the boundaries of the plate such that the appropriate voltages and current can be measured. The plate may be a metal plate as with the Hall effect or a more specific setup such as 2D graphene layer on an SiO_2 to observe the integer quantum Hall effect described in Sec 2.2.2.

The resulting resistances in the x direction (magnetoresistance) and y direction (Hall resistance) are given by $R_{xx} = \frac{V_x}{I_x}$ and $R_{xy} = \frac{V_y}{I_x}$, respectively.

2.2.2 Integer Quantum Hall Effect

The quantum Hall effect was discovered by Klaus von Klitzing in 1980 and has since been a key topic of research in many fields of physics. [20] It was first observed on the boundary between a semiconductor (Si-100) and an insulator (SiO_2). On this boundary there was a two-dimensional electron gas - i.e. the electrons were only free to move in the plane. By connecting contacts to measure the current in the x direction and voltage in the x and y direction, it is possible to record values at different magnetic flux strengths and measure its affect on the flow of electrons. Using different dirthis, experimectionsen in the ts found the resistance at the midpoint of the two dimensional boundary is given as

$$R_{xy}^{\nu} = \frac{V_y}{I_x} = \frac{h}{e^2 \nu}, \quad \nu = 1, 2, 3, ..., \tag{8}$$

where h is Planck's constant and e is the charge of an electron and ν are integers, known as the Landau filling factor, giving this phenomenon its name - the integer quantum Hall effect. [21]

These effects are due to two factors: the electrons are confined in two dimensions, and Landau quantisation - quantisation of cyclotron orbits of charged particles as a result of the magnetic field. At certain magnetic field strengths B_i, the Landau filling factor $\nu = \frac{nh}{eB} = i$ is an integer. At these values, the Fermi energy of the electrons (referred to as the chemical potential in Sec. 2.1.2) lies in an energy gap. Since there are no states available near the Fermi energy, the electrons state is considered to be incompressible, causing the magnetoresistance and Hall resistance to be quantised. In essence, the integer quantum Hall effect is the result of the quantisation of non interacting two dimensional electrons in a magnetic field.

2.2.3 Fractional Quantum Hall Effect

The fractional quantum Hall effect is an extension of the integer quantum Hall effect while measuring the Hall resistance of the two dimensional electron gas described in

2.2.2. Instead of occurring at integral Landau filling levels, this phenomenon now occurs, as the name suggests, at fractional level filling, where these fractions are rational numbers $\frac{p}{q}$. [22]

Unlike the integer quantum Hall effect, the fractional quantum Hall effect is the result of the motion of many two dimensional electrons in a magnetic field, all interacting with each other in their partially filled Landau levels. The properties of the fractional quantum Hall effect cannot be described by the single particle physics but instead the multi particle system creates the energy gaps of an inherently quantum nature - a quasiparticle system.

The magnetic field interacts with the many particle to create holes with a 2π phase twist, often denoted as a vortex. Each vortex has a charge given by the fractional filling of the Landau level. States where $\nu = \frac{1}{q}$, consist of electrons (charge e) surrounded by q holes - creating a quasiparticle. Since these quasiparticles are derived from fermions, their complete state has to be odd - requiring q to be an odd integer. These composite particles exactly cancel out the magnetic field - creating the observed effect at the fractional Landau level $\nu = \frac{1}{q}$.

At rational fractions sufficiently away from these states, the quasielectrons and quasiholes can form other quantum liquids (resisting changes in density, unlike fluids) - covering all fractions with odd denominators as well as some other even denominator fractions. [23]

Figure 5 shows the experimental data of the fractional quantum Hall effect experiment across a different range of magnetic field strengths. The plateaux in Hall resistance correspond to the dips in the magnetoresistance where the state is able to superconduct due to the vortices forming at these Landau filing levels. The dotted box labelled a) in the figure are between 2 and 3. This is where we find the levels $\frac{5}{2}$ and $\frac{12}{5}$. We will come to find that these levels are incredibly powerful for the purposes of quantum computing.
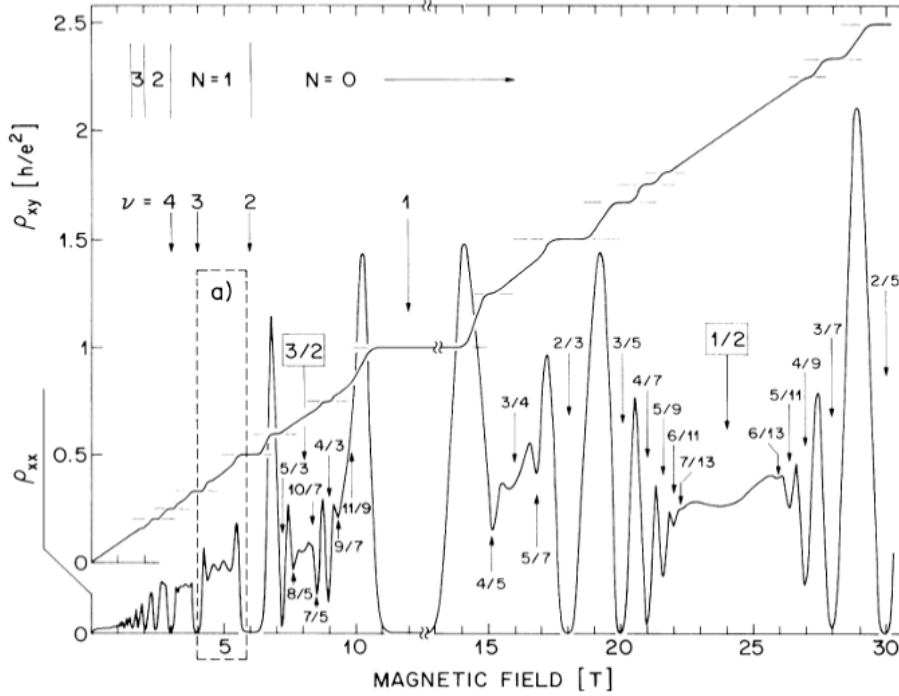
Figure 5: Experimental data showing the Hall resistance R_{xy}^{ν} and magnetoresistance R_{xx}^{ν} across a range of magnetic field strengths.[23]

3   Anyons

As research continued, investigating the statistics of quasiparticles in fractional quantum Hall systems, it was found that they exhibit neither fermionic nor bosonic statistics. Frank Wilczek found that exchanging two identical quasiparticles could give any phase [26], as opposed to 1 or -1 for bosons and fermions, respectively, coining them 'anyons' [25]. This can be apparent when looking at the rotations groups in two and three dimensions. [24]

In three dimensions, the rotation group SO(3) is a non-Abelian group with non trivial commutation relations. The Lie algebra of this group is proportional to the angular momentum operators for particles in three dimensions - directly implying a quantisation of $\frac{1}{2}\hbar$. Mathematically, the configuration space of two indistinguishable particles is given by $(\mathbb{R}_3 - \mathbf{0})/\mathbb{Z}_2 = \mathbb{R}P_2$ where we have subtracted the origin since we assume the paths of the particles don't cross and $\mathbb{R}P_2$ is the real projective plane. The first homotopy group π_1 records information about loops in a topology, and can be used to classify the group of all paths in the configuration space. We find that $\pi_1(\mathbb{R}P_2) = \mathbb{Z}_2$. Therefore the group

16

of elements are classified simply by $(1, -1)$ - fermions and bosons, respectively. [28]

Conversely, the two dimensional rotation group SO(2) is Abelian with trivial commutators. Therefore, the Lie algebra doesn't fix the angular momentum for a two dimensional system. Instead, it is quantised as $\hbar(\frac{\theta}{2\pi} + \text{integer})$, where θ is any real number. Mathematically, likewise with the three dimensions, the paths of the configuration space is given by $(\pi_1(\mathbb{R}_2 - \mathbf{0})/\mathbb{Z}_2) = \pi_1(\mathbb{R}P_1) = \mathbb{Z}$ where $\mathbb{Z}$ [28] is the group of integers under addition. Once again, this indicates that there is a large degree of freedom in the phases that an anyon may gain under exchange.

In general, there are two types of anyonic statistics that are observed. If the exchange of two anyons results in a complex phase $e^{i\theta}, \theta \neq 0, \pi$, the statistics is Abelian, describing *Abelian anyons*. On the other hand, if the exchange is described by non commuting $k \times k$ unitary matrices, the statistics describe *non-Abelian anyons* [28]. Since anyons arise in quantum Hall states, they are often denoted by the Landau filling fractions which creates to the anyon. Whilst most quantum Hall states produce Abelian anyons, there are certain filling fractions which give rise to non-Abelian anyons - as will be discussed in Sec. 3.2.

3.1   Abelian Anyons

Abelian anyons gain a complex phase upon exchange of two particles, explicitly:

$$|\psi_1\psi_2\rangle = e^{i\theta} |\psi_2\psi_1\rangle , \tag{9}$$

where θ cannot be 0 or π since returning to $|\psi_1\psi_2\rangle$ after another exchange must not lead to a phase of $2\pi n$. A phase of 0 would imply Bose-Einstein statistics and a phase of π would imply Fermi-Dirac statistics. In between, Abelian anyonic statistics is a one dimensional braid group B_n where n is the number of particles - this group will be outlined here and discussed in detail in Sec. 5.1.

Building a quantum mechanical model of such an exchange requires summing all paths that start and end in the same position - including any exchanges that occur since the

particles are indistinguishable. The total amplitude of such a model is given by

$$A = \sum_{\text{direct paths}} e^{iS} + e^{i\theta} \sum_{\text{one exchange}} e^{iS} + e^{2i\theta} \sum_{\text{two exchanges}} e^{iS} + ..., \tag{10}$$

where S is the action of the anyons. [27]

To construct the model we consider a spinless particle with a charge q which orbits around a solenoid along the z-axis at a distance $\mathbf{r}$. When there is no current flowing through the solenoid, the particle's angular momentum is quantised, as discussed previously - $l_z \in \mathbb{Z}$. However, when the solenoid has a current passing through it, an electric field is produced, affecting the particle such that

$$\int (\boldsymbol{\nabla} \times \mathbf{E}) d^2 \mathbf{r} = \int B d^2 \mathbf{r} = -\frac{\partial \phi}{\partial t}, \tag{11}$$

$$\int \mathbf{E} \cdot d\mathbf{l} = 2\pi |\mathbf{r}| E_\theta = \int B d^2 \mathbf{r} = -\dot{\phi} \implies \mathbf{E} = -\frac{\dot{\phi}}{2\pi |\mathbf{r}|} (\hat{z} \times \mathbf{r}). \tag{12}$$

The charged particle experiences a torque from the electric field resulting in a change of angular momentum

$$\dot{l}_z = \mathbf{r} \times \mathbf{F} = \mathbf{r} \times q\mathbf{E} = -\frac{q\dot{\phi}}{2\pi} \implies \Delta l_z = -\frac{q\phi}{2\pi}, \tag{13}$$

where Δl_z is the change in angular momentum due to the solenoid. Taking this model to a limit where the solenoid radius and the distance between the charged particle and the solenoid vanishes, a charged-fluxtube composite is created. In a planar system (no z direction), this composite becomes a point-like particle with fractional angular momentum - an anyon. So starting with a three dimensional spinless particle and adding topological restrictions causes the quasiparticles to have an intrinsic spin of $l_z = s_z = \frac{q\phi}{4\pi}$ - half of what was originally predicted since in a magnetic field the charge is directly proportional to the magnetic flux $q = c\phi(t)$. [27]

18

3.1.1 Many anyons states

We can look at the rudimentary picture of anyons we have built to create a more detailed model by studying how anyons interact with one another. [27] The Hamiltonian for a two identical anyon system is given by

$$\mathcal{H} = \frac{(\mathbf{p}_1 - q\mathbf{a}_1)^2}{2m} + \frac{(\mathbf{p}_2 - q\mathbf{a}_2)^2}{2m}, \tag{14}$$

where $\mathbf{a}_1$ and $\mathbf{a}_2$ are the vector potentials of the anyons due to the flux of the other anyon:

$$a_x = \frac{\phi}{2\pi} \frac{\hat{z} \times (\mathbf{r}_x - \mathbf{r}_y)}{|\mathbf{r}_x - \mathbf{r}_y|^2}. \tag{15}$$

Working in the centre of mass (COM) frame instead, we can define COM and relative coordinates as such

$$\mathbf{R} = \frac{\mathbf{r}_1 + \mathbf{r}_2}{2} \implies \mathbf{P} = \mathbf{p}_1 + \mathbf{p}_2, \text{ and } \mathbf{r} = \mathbf{r}_1 - \mathbf{r}_2 \implies \mathbf{p} = \frac{\mathbf{p}_1 - \mathbf{p}_2}{2}. \tag{16}$$

Therefore, in COM frame, the Hamiltonian is written as

$$\mathcal{H} = \frac{\mathbf{P}^2}{4m} + \frac{(\mathbf{p} - q\mathbf{a})^2}{m}, \text{ where } \mathbf{a} = \frac{\phi}{2\pi} \frac{\hat{z} \times \mathbf{r}}{|\mathbf{r}|^2}. \tag{17}$$

This Hamiltonian tells us that the COM frame moves as a free particle, however the relative motion is sensitive to the statistics of the particle. Since the quasiparticles have been formed using a bosonic particle in a bosonic flux, the wavefunction for relative movement of the two anyon system can be described best using polar coordinates symmetric under exchange.

$$\psi_{rel}(\mathbf{r}) = \psi_{rel}(-\mathbf{r}) \implies \psi_{rel}(r, \theta + \pi) = \psi_{rel}(r, \theta). \tag{18}$$

Performing a singular gauge transform such that

$$\mathbf{a}_{rel} \to \mathbf{a}'_{rel} = \mathbf{a}_{rel} - \boldsymbol{\nabla}\Lambda(r,\theta), \text{ where } \Lambda(r,\theta) = \frac{\phi}{2\pi}\theta, \tag{19}$$

simply reduces the Hamiltonian to $\mathcal{H} = \frac{\mathbf{P}^2}{2m} + \frac{\mathbf{p}^2}{2m}$ - the Hamiltonian for two free particles. [27] However, the relative wavefunction gains a phase - obeying anyonic statistics:

$$\psi'_{rel}(r, \theta + \pi) = e^{-iq\phi/2}\psi_{rel}(r,\theta). \tag{20}$$

By returning the the bosonic gauge, the wavefunction can now be solved in terms of the centre of mass wavefunction and the relative wavefunction, where the angular part gains the extra phase, and the radial part is simply the Bessel function. [27] Thus, the wavefunction for two anyons is

$$\psi(\mathbf{R}, \mathbf{r}) = \psi_{COM}(\mathbf{R})\psi_{rel}(\mathbf{r}) = e^{i\mathbf{P}\cdot\mathbf{R}}e^{i(l+q\phi/2m)\theta}J_{|l+q\phi/2m|}(kr). \tag{21}$$

However, since this ϕ can be any phase for anyonic statistics, this wavefunction can not be factorised into two one-particle wavefunctions, we must derive whether the energy levels can be obtained as the sum of two single particle energy levels. To do this, one must consider the particles in a potential. In this literature review we shall consider every physicists favourite potential - the harmonic oscillator. [28] Writing a standard harmonic oscillator potential for two particles and then changing coordinate system to COM and relative positions, the Hamiltonian is written as

$$\mathcal{H} = \frac{\mathbf{P}^2}{4m} + \frac{\mathbf{p}^2}{m} + m\omega\mathbf{R}^2 + \frac{1}{4}m\omega\mathbf{r}^2. \tag{22}$$

Solving this to find energy levels gives

$$E_{COM} = \omega(n + |L| + 1), \tag{23}$$

$$E_{rel} = \omega\left(n + \left|l + \frac{\alpha}{\pi}\right| + 1\right), \tag{24}$$

$$E_{2\,anyons} = E_{COM} + E_{rel} = \omega\left(2j + p + 2 \pm \frac{\alpha}{\pi}\right), \ \ p, j \in \mathbb{Z}, \tag{25}$$

were $\alpha = 0, \pi$ returns bosonic and fermionic states, respectively. [28]

Therefore, it is apparent that when α represents an anyonic state, the total energy level is once again not the sum of two single particle systems - so anyonic statistics are a complex system where systems require a more technical solution, whether they are in a free system or not. We can come to the conclusion that even free two anyon systems act as interacting ones due to statistical interactions.[28]

Many anyons systems work in a similar fashion, and they need to be treated as a set of multiple long-range statistically-interacting two-anyon system between all pairs of anyons. Mathematically we find that, for Abelian anyons, the fusion of two identical anyons of phase θ results in a bound state of phase 4θ. This accounts for both the angular momentum of each anyon, and the orbital angular momentum of the anyons with each other. Explicitly, the exchange of two anyons results in a phase of $e^{i\theta}$, however the exchange of two bound states (each containing two anyons) results in a phase of $e^{4i\theta}$. More generally, the exchange of two n-anyon bound states results in a phase of $e^{in^2\theta}$. The trivial particle in the anyon system is when particles of phase θ and $-\theta$ are bought together.

3.2 Non-Abelian Anyons

Non-Abelian anyons provide a different statistical model to Abelian anyons. As we will show, non-Abelian anyons have a degenerate ground state with a defined topological order - making them incredibly powerful for fault-tolerant quantum computation.

Physically, we can see what non-Abelian excitations look like by considering N de-

generate states represented by ψ_α, $\alpha = 1...N$, for N particles. Exchanging two particles provides a new wavefunction in the same degenerate space. Mathematically, $\psi = (\psi_1 \psi_2 ... \psi_N)^T \to \psi' = U\psi$ where U is a $N \times N$ unitary matrix. Exchanging two different particles will lead to $\psi \to \psi' = V\psi$, where V is also a unitary matrix of the same size. Requiring that U and V do not commute with each other provides the non-Abelian statistics required and clearly means that $N \geq 2$ since $U(1)$ is the group of commuting phases we previously discussed for Abelian anyons. We generalise the model of the Abelian anyon to the non-Abelian case by thinking of it as a charge orbiting a flux again. The charge moving around the flux and returning to its original position no longer picks up just a phase, but instead looks like

$$|q_i\rangle \to |q_i'\rangle = \sum_j U_{ij} |q_j\rangle, \tag{26}$$

where U_{ij} is the non-Abelian flux matrix. [27] However, unlike the Abelian case where the flux is path independent, the non-Abelian flux is path dependant. The basic requirements for a non-Abelian theory of anyons are the following

1. A list of the types of particles in the model

2. Fusion rules - rules for two anyons fusing and splitting (the inverse)

3. Rules for the braiding of particles (exchanging two particles)

Before specifying a particular set of rules as we will in Sec 3.2.1, it is important to set up a general framework to build on. To start building the model, we need a list of particles with their topological charges. By that we mean that the quasiparticle excitations are topological (e.g. $\mathcal{Z}_2$ charge) as opposed to local excitations (e.g. spin). The next step is defining the fusion algebra as

$$a \times b = \sum_c N_{ab}^c c, \tag{27}$$

where $N_{ab}^c \geq 0$ [27]. If $N_{ab}^c = 0$, the particle c is not produced, and if it is equal to 1 the particle is always produced. This is the case for Abelian models. However, for the

non-Abelian model $N_{ab}^c > 1$, i.e. the fusion of a and b has N_{ab}^c different ways of producing anyon c [27]. With this information of a general framework, we can now approach a defined non-Abelian model of anyons relevant to quantum computation.

3.2.1 Fibonacci Anyons

Fibonacci anyons are the simplest type of non-Abelian anyons, containing only two types - the trivial anyon $\mathbf{0}$ and the non-trivial anyon τ, with charge 1. We define the fusion rules as such

$$\mathbf{0} \otimes \mathbf{0} = \mathbf{0}, \tag{28}$$

$$\tau \otimes \mathbf{0} = \tau, \tag{29}$$

$$\mathbf{0} \otimes \tau = \tau, \tag{30}$$

$$\tau \otimes \tau = \mathbf{0} \oplus \tau, \tag{31}$$

where $\otimes$ is the act of fusion and $\oplus$ shows the sum of different possible results. [29]

Since the fusion of two Fibonacci anyons can result in the creation or annihilation of another anyon, the Fibonacci anyon is its own antiparticle - a Majorana particle. It is apparent that the number of possible outcomes - degenerate states - increases with the number of anyons according to the Fibonacci series (giving the anyons their name), and this will be shown in the next section.

The eigenvalues for the fusion matrix N_{ab}^c are known as the *quantum dimension* and dictate the probability of each result from the fusion of particles. The quantum dimension of τ particles is simply the golden ratio $d_\tau = \varphi = \frac{1+\sqrt{5}}{2}$. [29]

3.2.2 Degenerate ground states

Let us assume a many Fibonacci anyon state, where the anyons are brought together to fuse, how can we predict what the final product will be? Consider the simplest state of three well-separated Fibonacci anyons τ, where the first two fuse together they forming

either $\mathbf{0} \oplus \tau$. When the third anyon is bought in to fuse with this product, it will necessarily produce a τ if the first two resulted in the trivial anyon, else it will produce $\mathbf{0}$ or τ. Hence, if the final product is a τ anyon then there are multiple different paths that the fusion could've taken to get there. These are often represented by fusion trees, as shown below in Fig. 6.
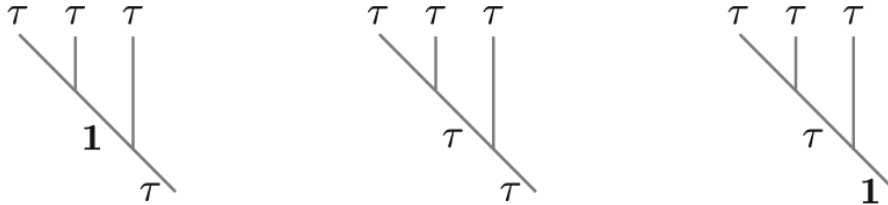

Figure 6: Fusion trees of three Fibonacci anyons [29]

In theory, given well-separated n anyons fusing together, any superposition of $\mathbf{0}$ or τ is possible, and these superposition will decohere into a particular anyon. By arranging these n anyons in a similar fashion to the three anyon ground state, we can build a fusion tree as before, fusing anyons from the left.

As will be visually shown when talking about braiding, the ground state manifold for a many anyon system is a degenerate state. This degeneracy is vital to use non-Abelian anyons to build a quantum computer and is a necessary result of the non-Abelian statistics.To provide a basis for these degenerate ground states, we can use the fusion trees we have introduced earlier and explore the different fusion paths that represent the same overall process.
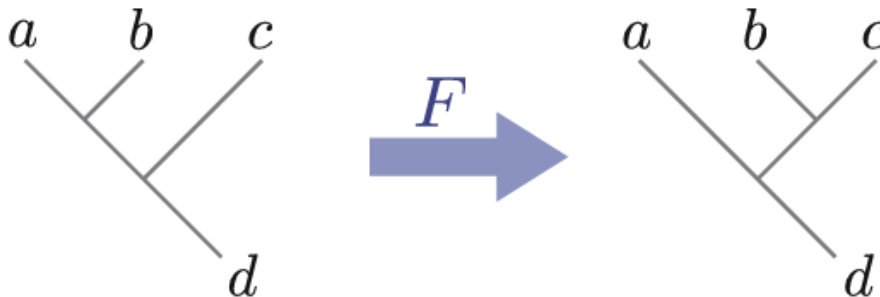

Figure 7: Different fusion trees for three anyons which lead to the production of the same anyon. These are related by an 'F move'. [29]

24

This fusion tree provides a combinatorial way to compute the degeneracy by counting the number of fusion paths. Labelling the ground state degeneracy as D_n and counting the degeneracies gives us $D_0 = 0$ and $D_0 = 1$. Then a simple proof by induction shows that $D_{n+1} = D_n + D_{n-1}$ - the Fibonacci series. The properties of the Fibonacci series establishes the quantum dimension to be φ for τ anyon and 1 for the **0** anyon. The probability to produce anyons i is given by the ratio between the quantum dimension of particle i d_i and the total quantum order $D = \sqrt{\sum_i d_i^2}$. Therefore when two anyons fuse, the probability to produce a **0** is $\frac{1}{\varphi^2}$, and probability for τ is $\frac{\varphi}{\varphi^2} = \frac{1}{\varphi}$. [29]

3.2.3 F Moves

In Fig. 7, there is a transformation that takes the left-hand diagram to the diagram on the right, represented by an F - called an F move. Since both fusion diagrams describe the same degenerate ground state, it must mean that the F move is represented by a unitary matrix - the F-matrix mathematically denoted as F_d^{abc}, where a, b, c are the anyons which will be fused and d is the resulting anyon. [29]

However, as we know from the degeneracy, with more anyons there will be many more different fusion trees and so a convention will be necessary for a consistent model. Fig. 8 illustrates F moves for a four anyon fusion tree, and it visually identifies the need to specify the change of basis matrices since the left most and right most fusion paths can be connected through two different paths.

The set of polynomial equations used to guarantee the consistency for the fusion trees is a mathematical theorem called the pentagons. Generally, these polynomial equations don't have a simple solution, however, due to Fibonacci anyons being self-dual (Majorana particles), the solution becomes more trivial. We find that if any of a, b, c, d are the trivial anyon **0**, then $F_d^{abc} = 1$. Therefore, the only non-trivial F-matrix is $F_\tau^{\tau\tau\tau}$, which is a 2×2 unitary matrix. [29]

However, even for Fibonacci anyons this leaves a lot of possible pentagons. For a four anyon fusion there are $2^5 = 32$, different pentagons due to the 5 anyons on the outer
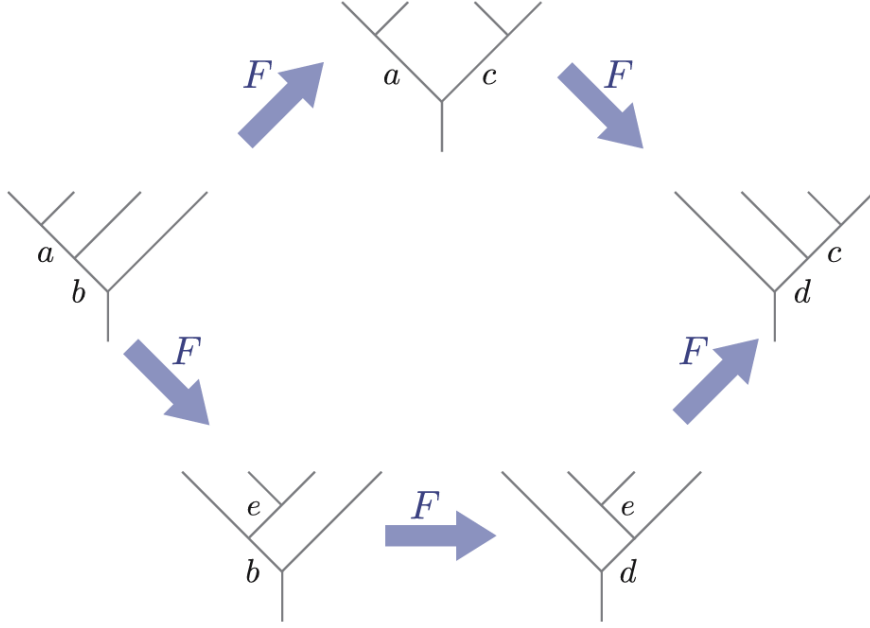
Figure 8: Pentagon relation for F-moves [29]

edges. However the only non-trivial pentagons are the ones with τ anyons on all 5 edges. To calculate this pentagon we need to order the fusion tree basis using Fig. 8 as below:

$$(F_\tau^{\tau\tau c})_a^d(F_\tau^{a\tau\tau})_b^c = (F_d^{\tau\tau\tau})_e^c(F_\tau^{\tau e\tau})_b^d(F_b^{\tau\tau\tau})_a^e, \tag{32}$$

where a, b, c, d, e label the inner edges of the fusion tree - shown in Fig. 8. By removing all trivial pentagons, we are left with

$$(F_\tau^{\tau\tau\tau})_1^1 = (F_\tau^{\tau\tau\tau})_\tau^1(F_\tau^{\tau\tau\tau})_1^\tau. \tag{33}$$

Finally, applying the constraint that F must be a unitary matrix, up to an arbitrary phase,

$$F_\tau^{\tau\tau\tau} = F_\tau^{\tau\tau\tau\dagger} = \begin{pmatrix} \varphi^{-1} & \varphi^{-\frac{1}{2}} \\ \varphi^{-\frac{1}{2}} & -\varphi^{-1} \end{pmatrix}, \tag{34}$$

where φ is the golden ratio. [29]

For now, this is all we will say about Fibonacci anyons. However, after quick mathe-

matical aside, we shall promptly return to discussing the properties of these quasiparticles which make them so useful for quantum computation.

4 Knot Theory: A Mathematical Aside

Before progressing to look into the intricacies of building quantum algorithms using a topological quantum computer, it is important to understand why non-Abelian anyons are even useful to build them. As mentioned, a two dimensional anyonic system is tolerant to any local changes and requires a topological change in order to create a different degenerate state.

Anyonic braiding is mathematically identical to knotting. If a system can be rearranged without exchanging any particles then it is the same degenerate state. Likewise, if a knot can be rearranged without cutting the string, it is the same knot. In this mathematical aside, we will delve into the specifics of this idea.

First, we need to define a knot. A knot is defined in mathematics as an embedding of a circle S^1 into a three dimensional space $\mathbb{R}^3$ [30]. Since the embedding is of a circle, unlike a conventional knot, a mathematical knot is closed instead of having open ends. Mathematical knots also have no thickness and so don't display any characteristics of physical friction. A knot with a thickness is called a framed knot and it is an embedding of a torus $D^2 \times S^1$ into $\mathbb{R}^3$.

For the purposes of topological quantum computing we will be looking exclusively at tame knots. These are knots whose image in $\mathbb{R}^3$ is made up of a finite amount of line segments, and all equivalent knots [30]. The most simple knot is the trivial knot or the unknot - a round circle embedded in $\mathbb{R}^3$. Examples of non-trivial knots are the trefoil knot and a cinquefoil knot, pictured in Fig. 9.

4.1 Reidemeister Moves

Reidemeister moves are the complete set of operations one can implement on any given knot to leave it invariant. It was shown in 1927 by Kurt Reidemeister [32] that any two diagrams representing the same knot can be related to one another through a finite sequence of just three different moves - the Reidemeister moves. Each move acts on just
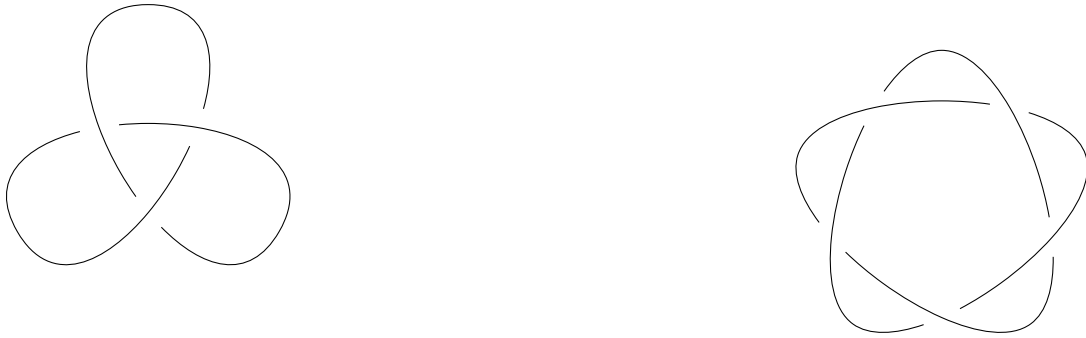
Figure 9: Right) Trefoil Left) Cinquefoil

a small finite region of the knot and are as follows

   I. Twist or untwist in their direction

  II. Move one loop complete over another

 III. Move a string completely over or under a crossing

Here, the ordering is also a label representing the number of strands involved in the Reidemeister move.

4.2 Knot invariants

While it is evident that the two knots in Fig. 9 do not look alike, one cannot be certain that these two knots cannot be modified, without cutting the string, to look like each other. Whether or not two knots are equivalent or not is an incredibly important topic with multidisciplinary applications, not only to the topics of topological quantum computing but even sciences like DNA biology. [45]

To identify equivalent knots, we must find a quantity which is the same for all equivalent knots and remains invariant under any Reidemeister moves - called knot invariants.

4.2.1 Kauffman Polynomial

The Kauffman invariant is a result given by the Kauffman polynomial [33] - where two topologically equivalent knots will give the same value [31]. The Kauffman invariant is calculated by un-knotting the knot until there are only unknots left - like so:

Figure 10: Kauffman Rules

These sets of transformations are applied to every cross that exists on a knot in order to separate them, gaining a coefficient as they go along. Every unknot from each step can then be removed by replacing it with the coefficient d. To demonstrate how such a process works, we shall find the Kauffman invariant of the trefoil. Fig. 11 is a diagram which goes step by step into breaking down the trefoil knot using the rules and by adding the coefficients as we go along. The blue diagrams show the unknotted final diagrams which would be summed together to find the final Kauffman invariant. Hence the final value for the trefoil is $\frac{1}{A}d^2 + Ad + Ad + A^3d^2 + Ad + \frac{1}{A}d^2 + \frac{1}{A^3}d^3 + \frac{1}{A}d^2$. Expanding and simplifying this expressions leads to the Kauffman invariant being $A^7 + A^3 + \frac{1}{A} - \frac{1}{A^9} = (A^{-7} - A^{-3} - A^5)d$. However, it can be seen that more complicated knots require exponentially more steps to calculate the Kauffman invariant. More precisely, a knot with n intersections requires 2^n terms to be calculated. [31]

For now we will leave this mathematical aside on knot theory here, and return to studying anyons, where we will apply the results of knot invariants to topological systems in quantum computing.
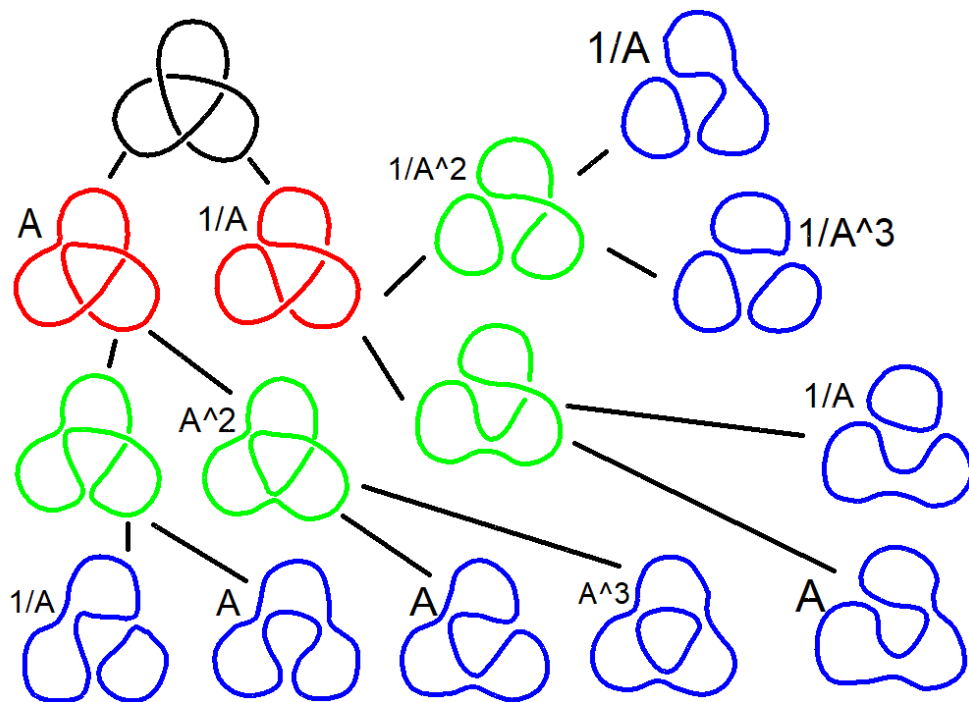
Figure 11: A step by step visual demonstration of the method used to calculate the Kauffman invariant of the trefoil. Each colour symbolises the splitting of an intersection using the method described in Fig. 10.

5   Braiding

To understand braiding we must define what we mean by a topological quantum theory. In a topological quantum field theory (TQFT), the probability amplitudes of a given system depend only on the topology of the process and not on the detailed geometry. [31] Diagrammatically represented:
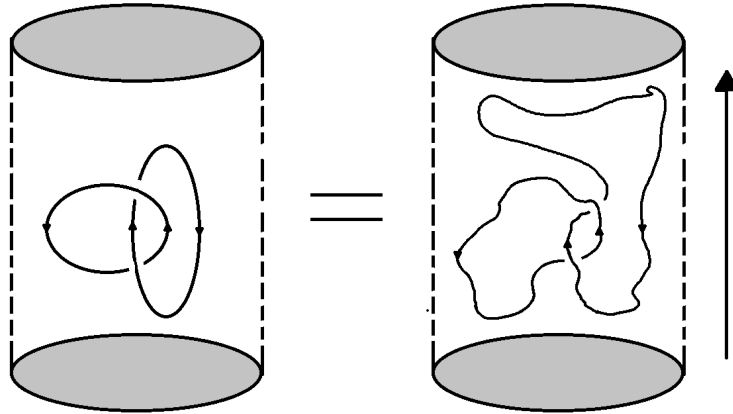

Figure 12: Paths of two particle-hole pairs in a two dimensional plane, travelling along time as indicated by the arrow on the right. Both diagrams are topologically invariant

Consider a 2D plane as shown in gray in Fig. 12, which travels up in time, indicated by the world line on the right of two images. At certain points in time, a particle and its corresponding hole are produced from the vacuum and they travel through the 2D plane until they annihilate later on with each other. During this process, they wrap around the another particle-hole pair. The diagram shows that while the paths of the two images are wildly different, they represent the same system, because a TQFT only depends on the topology and not the detailed geometry. Visually, one can comment on the likeness of this scenario with knot invariants discussed in the previous section.

Edward Witten discovered in 1989 that the amplitude of a process is given by the Jones Polynomial [34] - a special case of the Kauffman polynomial - of the knot. However to define this relation we must link the mathematical theory of knot invariants to a physical topological invariance. Mathematically, a topological invariant is something that can be calculated from a manifold $\mathcal{M}$, without defining a metric. A quantum field theory which

is defined on a manifold without a defined metric is said to be 'generally covariant' or sometimes 'background independent'. [34] More precisely, general covariance refers to the theory respecting the symmetry of diffeomorphism invariance in manifest way.

The most common generally covariant or diffeomorphism invariant quantum field theory is found in general relativity coupled to matter, where a metric is introduced, and then we integrate over all metrics. Here the action is diffeomorphism invariant by virtue of the transformation of the fields and metric. Since all metrics are integrated over in a path integral sense, a priori there is no preferred metric.

However, the 1989 paper by Edward Witten utilises methods from Jones to create quantum field theories which are generally covariant/diffeomorhism invariant in a trivial way, as the action can be defined without specifying a metric, in terms of topological invariants, specifically a Chern-Simon term. This is the sense in which the quantum field theory is topological. Using this method, Michael Freedman, a prominent mathematician in the field of TQFT, postulated that if a lab could create such a system which follows TQFT, measuring amplitudes of processes would give us the ability to calculate the Jones Polynomial or Kauffman invariant of a knot. This allows us to compute a exponentially hard mathematical problem, in polynomial time - proving the computational power that TQFTs may have once constructed. [35]

As mentioned in Sec. 3.2.2, non-Abelian anyons have degenerate ground states. Visually, this can be seen in Fig. 13 where the same ground orientation of particles in both the left and right hand images can be produced from two different, inequivalent histories. Therefore it can be seen that these are two degenerate ground states [31].

However, as figure 14 shows, a simple braid between two particles results in the production of the second ground state. Thus allowing us to come to the conclusion that braiding anyons transitions the state to a different degenerate ground state [35].

However, this leads us to ask the question that, given a state, how do we know which ground state it is without knowing it's history? By representing the left and right hand states in Fig. 13 as kets $|GS_2\rangle$ and $|GS_1\rangle$, respectively, we can define their corresponding
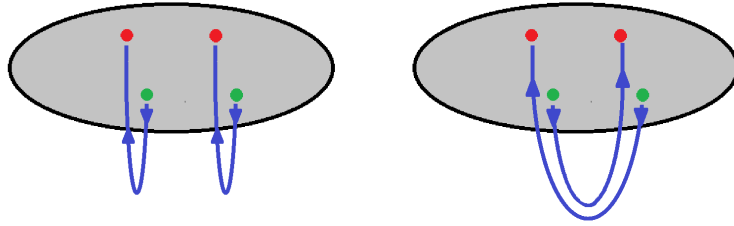
Figure 13: Two identical looking ground states with different space-time histories created by two pair productions from the vacuum on a two dimensional plane with time travelling upwards.
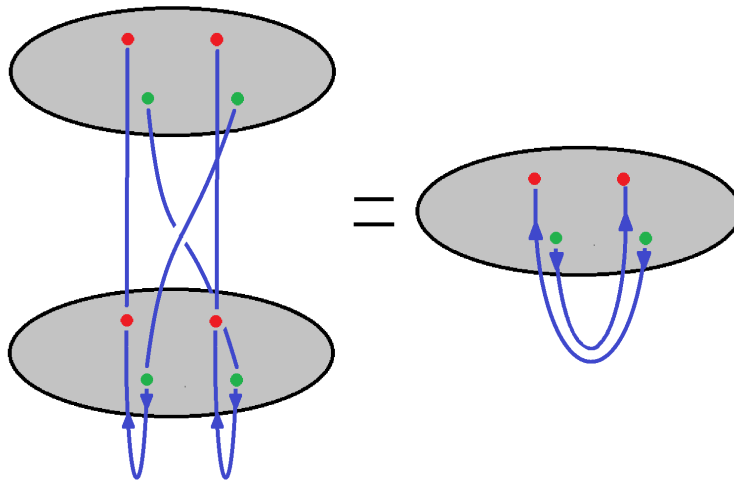

Figure 14: Braiding the two lower particles in the left ground state puts all particles in the same arrangement as the ground state on the right - making them equivalent ground states. Braiding particles with each other changes the ground state of the system.

bras. By acting the bra on a ket to find the probability amplitude, as shown in Fig. 15), we can find the amplitudes of such a process occurring. To find this amplitude, we can employ the Kauffman polynomial as before, and find that different ground states produce different results - allowing us to identify the various degenerate ground states of our non-Abelian anyonic system.

Fig. 15 shows the two degenerate ground states that have been discussed so far - this time also represented mathematically as a pair of kets $|GS_1\rangle$ and $|GS_1\rangle$. These ground states are produced through pair production of a particle and a hole. The corresponding bras of these ground states are then, a particle and hole pair annihilating into the vacuum.
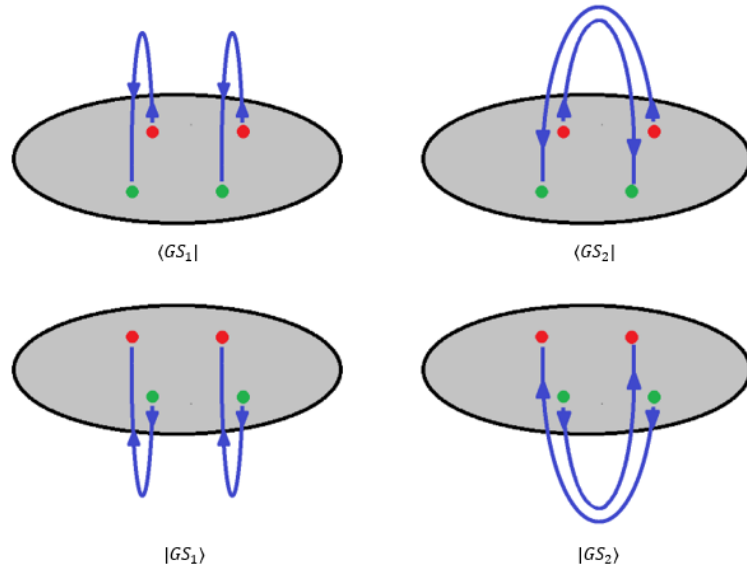
Figure 15: Flipping the ground states shows the particles travelling up and fusing back to the vacuum. This represents the 'ket' of the system. These can be joined with the 'bras' of the ground states to find the probability of the system evolving as shown by the diagram.

Fig. 16 enables us to visually see what happens when the bras and kets introduced before are used to find the amplitude of the different ground states. We can see that, if the same ground state is in both the bra and ket, we get two unknots, meaning the amplitude is d^2. Furthermore, for this simple example, if the ground states are mixed then we get one unknot so the amplitude is simply d. Ensuring that $d \neq 1$, it is possible for us to distinguish between different degenerate ground states.

From the images in Fig. 16 it can be seen that no local operators can cause transition between the ground states, and only by braiding - a global operator - can the ground state be transformed. Thinking back to quantum computers, we can see that this is the incredibly appealing property of topological quantum field theories that enables a fault-tolerant quantum computer to be possible. [35]

However, the final piece of the puzzle remains - we haven't defined what the Kauffman polynomial value A is, and therefore what d is. When introducing non-Abelian anyons, we discussed that they arise from specific fractional quantum Hall states which have non-Abelian statistics, and that they were represented by their Landau filling level. These
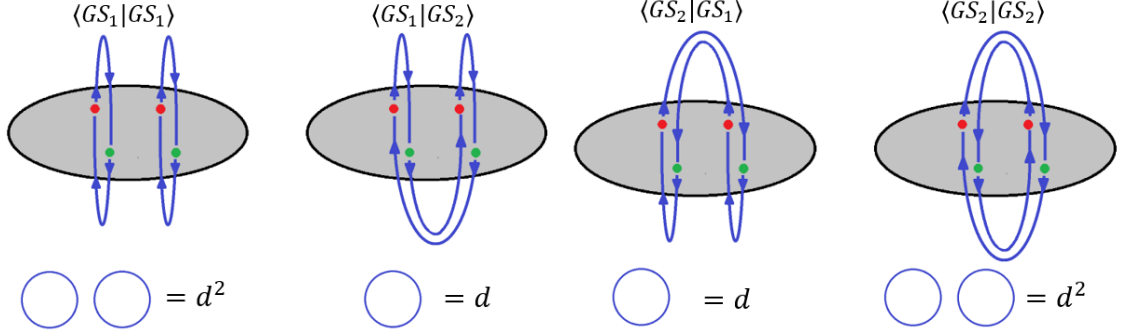
Figure 16: Amplitudes of degenerate ground states

fractional values are essential in defining the A for our knot invariant theory, completing the model and allowing us to make measurements of amplitudes and, in turn, specify transitions between ground states.

The two most common non-Abelian FQHE states that scientists look at for their uses in quantum computing are the $\frac{5}{2}$ state, Ising anyons, and $\frac{12}{5}$ state, Fibonacci anyons, due to their high mobility. The $\frac{5}{2}$ state has a non-Abelian unitary symmetry of $\mathrm{SU}(2)_2$ which gives it a Kauffman invariant value $A = ie^{i\pi/2(2+2)} = ie^{i\pi/8}$, while the $\frac{12}{5}$ state has a non-Abelian unitary symmetry of $\mathrm{SU}(2)_3$ which gives it a Kauffman invariant value $A = ie^{i\pi/2(2+3)} = ie^{i\pi/10}$. [31]

5.1   R-moves

Given n anyons a_i in well separated, fixed positions x_i on a two dimensional surface S, we can construct the degenerate ground states as $V(S; x_i, a_i)$, $i = \{1, ..., n\}$ [29]. Exchanging two well separated anyons a_i, a_j adiabatically will maintain the ground state manifold. Letting the initial ground state be $|\Psi_0\rangle \in V(S; x_i, a_i)$, then after the braiding of two particles, the system will be in another ground state $|\Psi_1\rangle = \sum_i \varphi_i e_i \in V(S; x_i, a_i)$, where we define a metric such that e_i is an orthonormal basis for our manifold. By running $|\Psi_0\rangle$ over this basis, we map $V(S; x_i, a_i)$ to itself using a unitary matrix we shall refer to as $R_{i,j}$ [29]. If S, our surface, is a disk - as we have defined it to be, then this representation of the mapping class group is the 'braid group' B_n. We should note that it is possible to choose a basis e_i such that $R_{i,j}$ is a diagonal matrix.

As we have explored, clockwise and anticlockwise braiding produce two different ground states due to the difference in the Kauffman rules, therefore it is necessary to define a convention for braiding. We will define the exchange of two particles as an anticlockwise exchange (right handed), and the inverse operation with will be a clockwise exchange (left handed).

The other conjugate transformation that we can apply to anyon transformation is to the F matrix we introduced earlier. The converse of two anyons fusing is the splitting of an anyon to produce two anyons. Therefore, as time goes upwards in our R-matrix convention, a fusion tree can be interpreted as a 'splitting' tree [29]. In fact, all braiding between anyons can be described using combinations of R-moves and F-moves, or mathematically, all braiding matrices can be constructed from R-matrices and F-matrices.

Let the ground state manifold of the fusion tree for anyons a, b fusing to anyon c: $V(S; x_i, a_i)$ be written as $V_c^{a,b}$ with a basis $e_c^{a,b}$. When the two anyons undergo braiding under the R move $R_{a,b}$, the basis $e_c^{a,b}$ undergoes a transformation $R_{a,b}e_c^{a,b}$, now in a ground state manifold of $V_c^{b,a}$. This new state is now represented by an R-matrix $R_c^{b,a}$. [29] Diagrammatically, this is shown in Fig. 17

Figure 17: How an R move changes the degenerate ground state of a system. [29]

Consider two anyons c, d where d splits into a, b, after which c braids first with a and then with b. Conversely, imagine c, d first braid with each other before splitting into a, b. It is clear that there are equivalent ground states and can be transformed into one another through the series of moves in Fig. 18.
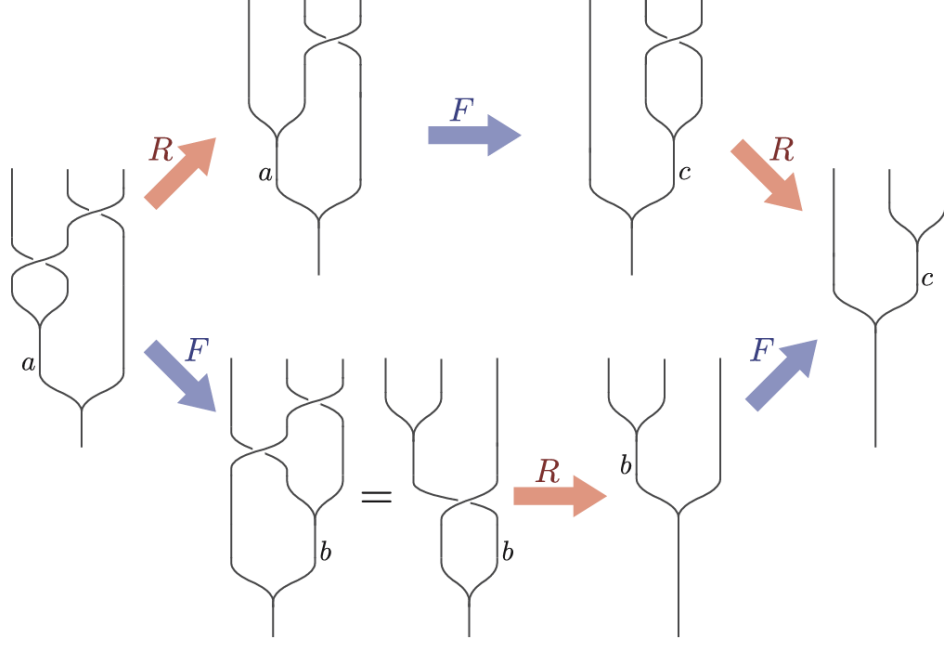
Written mathematically,

Figure 18: hexagon relation for two states through R-moves and F-moves. [29]

$$R_c^{\tau,\tau}(F_\tau^{\tau\tau\tau})_a^c R_a^{\tau,\tau} = (F_\tau^{\tau\tau\tau})_b^c R_\tau^{\tau,b}(F_\tau^{\tau\tau\tau})_a^b, \tag{35}$$

where, like with F-moves, the labels a, b, c represent the inner edges of the system [29]. Once again, we can observe that braiding an anyon τ around the trivial anyons $\mathbf{0}$ is trivial i.e. $R_\tau^{0,\tau} = R_\tau^{\tau,0} = 1$. Substituting in the F-matrix from Eq. 34 for Fibonacci anyons, we find that the transformation becomes

$$\begin{pmatrix} (R_0^{\tau,\tau})^2\varphi^{-1} & R_0^{\tau,\tau}R_\tau^{\tau,\tau}\varphi^{-\frac{1}{2}} \\ R_0^{\tau,\tau}R_\tau^{\tau,\tau}\varphi^{-\frac{1}{2}} & -(R_0^{\tau,\tau})^2\varphi^{-1} \end{pmatrix} = \begin{pmatrix} R_0^{\tau,\tau}\varphi^{-1} + \varphi^{-2} & (1 - R_\tau^{\tau,\tau})\varphi^{-\frac{3}{2}} \\ (1 - R_\tau^{\tau,\tau})\varphi^{-\frac{3}{2}} & R_0^{\tau,\tau}\varphi^{-2} + \varphi^{-1} \end{pmatrix}, \tag{36}$$

which has the solution [29]

$$R_0^{\tau,\tau} = e^{4\pi i/5}, \quad R_\tau^{\tau,\tau} = e^{-3\pi i/5}. \tag{37}$$

Therefore, the process of braiding two anyons together requires a basis transformation F, followed by braiding the particles together using an R-matrix - often called a braid-matrix defined as $B = F_c^{a\tau\tau}R_{\tau,\tau}F_c^{a\tau\tau}$. Visually, applying a B-move will affect as system

in the following way

Figure 19: braiding of two identical anyons [29]

We can create a basis in Dirac notation - $\{|abc\rangle\}$ - by looking at the edges adjacent labelled a, b, c, as before, and using the fusion rules as outlined [29]. Before the basis transformation due to the F move, the basis is as follows

$$|\mathbf{0}\tau\mathbf{0}\rangle, |\tau\tau\mathbf{0}\rangle, |\mathbf{0}\tau\tau\rangle, |\tau\mathbf{0}\tau\rangle, |\tau\tau\tau\rangle, \tag{38}$$

then after the basis change to $\{\left|a\tilde{b}c\right\rangle\}$, the basis becomes

$$|\mathbf{000}\rangle, |\tau\tau\mathbf{0}\rangle, |\mathbf{0}\tau\tau\rangle, |\tau\mathbf{0}\tau\rangle, |\tau\tau\tau\rangle. \tag{39}$$

The F-matrix in the representation given by the basis is

$$F = \begin{pmatrix} 1 & & & & \\ & 1 & & & \\ & & 1 & & \\ & & & \varphi^{-1} & \varphi^{-\frac{1}{2}} \\ & & & \varphi^{-\frac{1}{2}} & -\varphi^{-1} \end{pmatrix}, \tag{40}$$

and the R-matrix in this representation is

$$R = \mathrm{diag}(e^{4\pi i/5}, e^{-3\pi i/5}, e^{-3\pi i/5}, e^{4\pi i/5}, e^{-3\pi i/5}), \tag{41}$$

which allows us to calculate the braid matrix [29]

$$B = FRF^{-1} = \begin{pmatrix} e^{4\pi i/5} & & & & \\ & e^{-3\pi i/5} & & & \\ & & e^{-3\pi i/5} & & \\ & & & \varphi^{-1}e^{-4\pi i/5} & \varphi^{-\frac{1}{2}}e^{-2\pi i/5} \\ & & & \varphi^{-\frac{1}{2}}e^{-2\pi i/5} & -\varphi^{-1} \end{pmatrix}. \quad (42)$$

With mathematically rigorous matrix representations of transformations regarding anyon interactions, it is now possible to create quantum gates from these interactions and create a explicit model of quantum computation through the braiding of Fibonacci anyons.

5.2 TQC with only one mobile quasiparticle

In March 2006, a paper was published by the same leading researchers in the field of topological quantum computing which would once again illustrate how powerful this theory could be if put into practice. The paper proved, as we will go on to discuss, that any quantum computation which is done through braiding n identical quasiparticles, in our case Fibonacci anyons, can be performed by braiding a singular anyon (the *warp* anyon) around $n - 1$ other fixed identical anyons (the *weft* anyons). [36] This is an especially powerful discovery since, in practice, it is much easier to manipulate one anyon instead of many. Not only does it make the method more reliable, but increases the potential of a larger, many qubit system. [36]

The subgroup of braids B_n in which only one particle is moving, while the others remain in fixed position is known as the weave group W_n. Below in Fig. 20 from the original paper, where the convention is for time to travel from left, is an example of this.

To construct the model of a one anyon group we define a subgroup of the braid group B_n called the 'purebraid' group on n anyons - PB_n. This group braids the particles such that all the anyons start and end in the same position after undergoing braiding. We can now create a normal subgroup of PB_n known as 'pureweaves' on n-1 weft particles
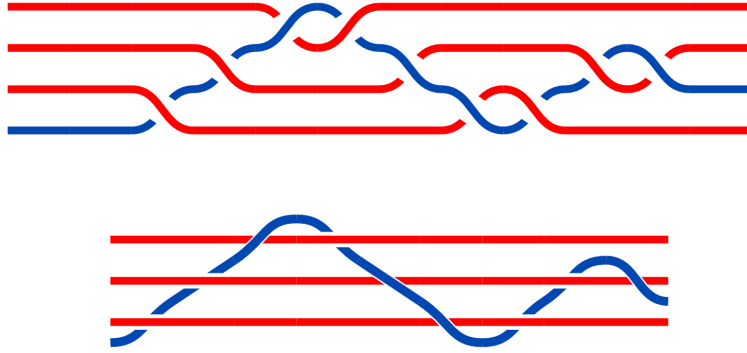
Figure 20: A progression of braids redrawn as a weave instead [36]

PB_{n-1} [36]. The theory defines this as analogous to weaves on the weft anyons where the warp particle starts and ends at the same position. Since PW_{n-1} is a normal subgroup. we can choose any $b \in PB_n$ and $w \in PW_{n-1}$ such that bwb^{-1} is topologically equivalent to a pureweave. This is visually shown in Fig. 21 also from the original paper:
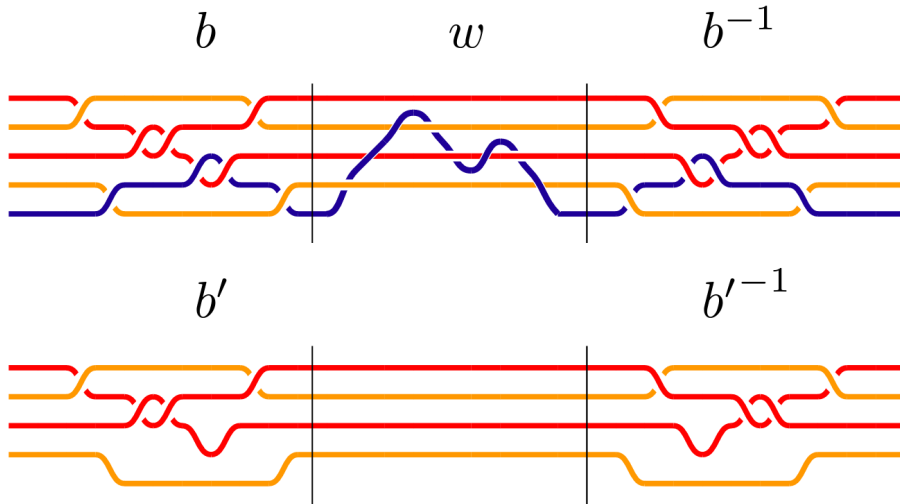

Figure 21: Visual proof that PW_{n-1} is a normal subgroup of PB_n. The top image demonstrates a purebraid b of 5 anyons followed by a weave w with 4 fixed weft anyons and one warp particle, followed by the inverse purebraid b^{-1}. Removing the warp particle completely, shown in the bottom image, results in the identity, therefore bwb^{-1} must also be a weave. [36]

Considering a topological system of n identical Fibonacci anyons and a Hilbert space of dimension M, it has been shown that for this system there exists a 'dense image' for the purebraids PB_n of this system in a space called $PU(M) = SU(M)/\mathbb{Z}_M$ [36]. This means that for any $a \in PU(M)$, there exists a $b \in PB_n$ which maps to a $\tilde{a} \in PU(M)$

which is arbitrarily close to a. [36]

Since, PW_{n-1} is a normal subgroup of PB_n, it reasons to follow that it must also have a dense image which is a normal subgroup of $PU(M)$. However, $PU(M)$ only has two known subgroups, the identity, and the entire group. It is trivial to see that not all pureweaves do not map to the identity, given the nature of all calculations we have done so far, hence it is apparent that PW_{n-1} must also have a dense image in all of $PU(M)$ [36]. Therefore, any braiding process can be approximated to a weave with arbitrary accuracy.

A very important weave to enable one anyon to braid with all the anyons as required is the injection weave. The injection weave for the Fibonacci model approximates to the identity operation on the Hilbert space to better than one part in a hundred and allows the warp anyon to travel across two weft anyons without changing the system [36] . This enables the warp anyons to travel across the system and braid with all the particles necessary. An example of this is shown in Fig. 22, where the injection weave in represented by the grey box.

Therefore, with the constraint that the injection weave is only approximately the identity, it is possible to perform any anyonic braid between n anyons as one singular warp anyon weaving in between $n - 1$ stationary anyons. Although this requires many more swaps between particles than braiding them would require, it is still much easier from a practical standpoint to perform a long operation provided there is only one anyon to be moved. The reasoning of this becomes fairly obvious when we consider that an anyon is an quasiparticle built out of charged vortices in a two-dimensional plane exhibiting the FQHE. Equipped with this model, we can finally build quantum gates to perform quantum computations.

$$\tau_2 \quad \tau_5 \quad \tau_4 \quad \tau_3^{-2} \quad \tau_1^{-1}$$

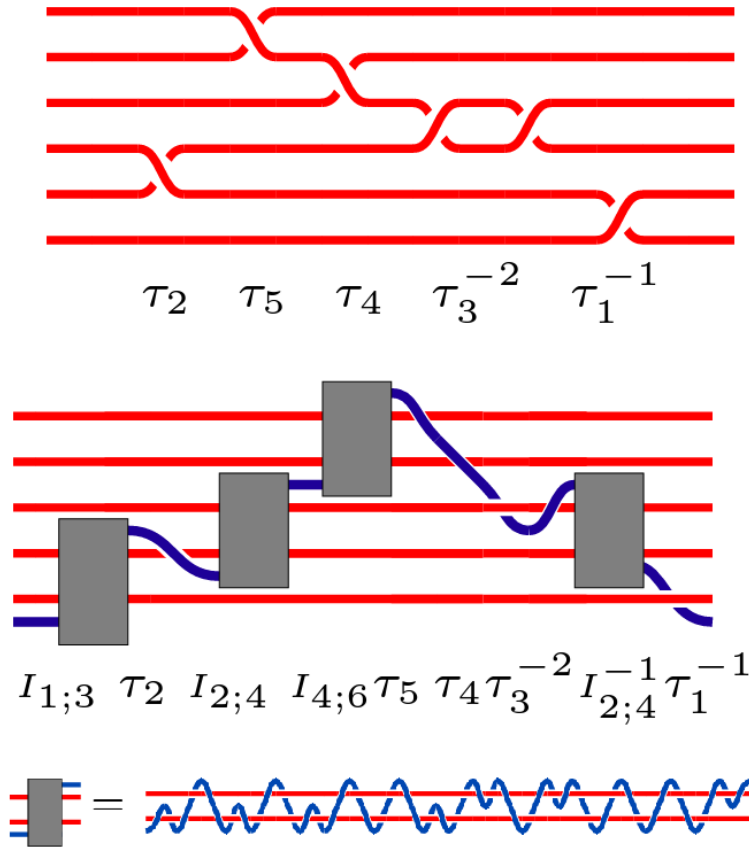$$I_{1;3} \ \tau_2 \ I_{2;4} \ I_{4;6} \tau_5 \ \tau_4 \tau_3^{-2} I_{2;4}^{-1} \tau_1^{-1}$$

Figure 22: Instead of braiding all 6 anyons with each other, the injection weave enables the warp anyon to move between the weft anyons to perform the braids itself, resulting in the same process. The third image shows the injection what the injection weave involves. [36]

5.3 Quantum Gates from Braiding

5.3.1 Classical Gates

To perform a computation, a classical computer utilises gates which prohibit or allow the flow of current - represented by a 1 or a 0 in a code for a certain operation. Examples of such gates are

- AND gate - if inputs a and b are both 1, then the output is 1, else the output is 0.

- OR gate - if either or both inputs a and b are 1, then the output is 1, else it is 0

- NOT gate - if the input a is 1 the output is 0, and vice versa

- XOR gate - if either but not both inputs a and b are 1, then the output is 1, else it is 0.

A sequence of these operations is read from left to right with brackets given priority, where an AND gate is represented using a $\cdot$, OR and XOR gates are represented using $+$ and $\oplus$, respectively, and NOT gates are shown using an line over the input $\bar{a}$. The results of a sequence of logic gates can be calculated using a truth tables. An example is shown below for the operation $\overline{a \cdot b} \cdot (a \oplus \bar{c})$, for all possible inputs $|abc\rangle$.

a	b	c	$a \cdot b$	$\overline{a \cdot b}$	$\bar{c}$	$a \oplus \bar{c}$	$\overline{a \cdot b} \cdot (a \oplus \bar{c})$
0	0	0	0	1	1	1	1
0	0	1	0	1	0	0	0
0	1	0	0	1	1	1	1
0	1	1	0	1	0	0	0
1	0	0	0	1	1	0	0
1	0	1	0	1	0	1	1
1	1	0	1	0	1	0	0
1	1	1	1	0	0	1	0

However, as you can see, these operations are not reversible since the same final output can have more than one initial input. In this example, all of $|000\rangle$, $|010\rangle$ and $|101\rangle$ result in an output of 1. Therefore we can make the statement that classical logic gates are not reversible. However, quantum gates are reversible, meaning they never lose information throughout their process. Therefore, a different array of quantum gates must be created that differ to the gates for a classical computer. These gates must be reversible, while still allowing us to create algorithms to perform computations.

5.3.2 Qubits

The aspect of quantum computing that makes it more powerful than a classical computer is the ability to create a superposition between the orthonormal states $|0\rangle$ and $|1\rangle$. This

lends itself to perform quantum computations through the methods of linear algebra with gates being matrices which transform the vector state of a qubit. It is convention to represent $|0\rangle = (1,0)^T$ and $|1\rangle = (0,1)^T$, although a different set of orthonormal basis can be created in other systems. The requirement of the orthonormal basis is that they are the eigenstates of the system, so that a measurement of the system will result in either one of the two states.

Combining multiple qubits to perform quantum computations is done the same way it would be done in linear algebra - through a tensor product - producing a superposition between the 4 states you would expect from a classical computer:

$$|0\rangle \otimes |0\rangle = |00\rangle = \begin{pmatrix} 1 \\ 0 \\ 0 \\ 0 \end{pmatrix}, \quad |0\rangle \otimes |1\rangle = |01\rangle = \begin{pmatrix} 0 \\ 1 \\ 0 \\ 0 \end{pmatrix}, \tag{43}$$

$$|1\rangle \otimes |0\rangle = |10\rangle = \begin{pmatrix} 0 \\ 0 \\ 1 \\ 0 \end{pmatrix}, \quad |1\rangle \otimes |1\rangle = |11\rangle = \begin{pmatrix} 0 \\ 0 \\ 0 \\ 1 \end{pmatrix}. \tag{44}$$

A pair of qubits can be in a normalised superposition of any of these four basis eigenstates, in a space $\mathbb{C}^{2^2} = \mathbb{C}^4$, however, if a state with qubits $|\psi_1\rangle$ and $|\psi_2\rangle$ can be written as $|\psi_1\rangle \otimes |\psi_2\rangle$, then this state is considered separable and in the subspace $\mathbb{C}^{2 \cdot 2} = \mathbb{C}^4$. In general, for n qubits, there is a subspace of $\mathbb{C}^{2n}$ of separable states in total space of $\mathbb{C}^{2^n}$ [37]. All states outside of this subspace are entangles states, and they are key to quantum computation because measurement of any qubit in an entangled state will provide information about the states of all entangled qubits.
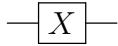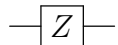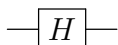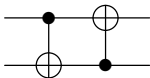
5.3.3 Quantum Gates

In a classical computer, the output of a gate results in a new input which can be fed into a new gate. However, this results in the loss of information as these gates are not reversible. On the other hand, quantum systems store information in a qubit 'register' which are simply transformed to different states under the rules of linear algebra through the use of unitary matrices. Thinking back to braiding matrices, we should remember that both R-matrices and F-matrices are unitary matrices, meaning that braiding does not violate any rules required for creating quantum gates.
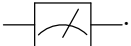
Earlier we showed that n qubits create a basis of dimension 2^n, meaning that quantum gates are of the size $2^n \times 2^n$. However, most gates will act on only one or two qubits at a time, therefore any unaffected qubits will simply by multiplied by an identity operator in that gate. For example, a gate U acting on the third qubit of a 4 qubit state will be created as $\mathbb{I}_2 \otimes \mathbb{I}_2 \otimes U \otimes \mathbb{I}_2$, where U is a unitary 2×2 matrix. There also exist, 'controlled gates', where the state of one qubit affects the state of another - and will typically entangle these two qubits together [3]. Controlled gates are of the form

$$|0\rangle \langle 0| \otimes \mathbb{I}_2 + |1\rangle \langle 1| \otimes U = \begin{pmatrix} 1 & 0 & 0 & 0 \\ 0 & 1 & 0 & 0 \\ 0 & 0 & U_{00} & U_{01} \\ 0 & 0 & U_{10} & U_{11} \end{pmatrix}. \tag{45}$$

The most common and useful quantum gates are shown in the table below. The NOT gate works in a similar fashion to the classical NOT gate, however in this case it swaps the probabilities of the qubit being found in that particular state. The Pauli Z gate flips the phase of the qubit, and while that has no effect on the probability of the state, it can affect interactions later on in the circuit. It is apparent that applying these gates once more to the system will return it to its original form - i.e. they are Hermitian. The next gate is the Hadamard gate, this simply puts a qubit into a superposition of both it's states, allowing it to take part in quantum computations. The CNOT and CCNOT gates

are extensions of the NOT gate, where the state of the control gate affects the outcome of the target gate. There are many gates not included in the list but can be useful in a circuit such as SWAP gates, anti-CNOT gates, ROT gates and Pauli Y gates.

Name	Matrix	Symbol
NOT (Pauli X, bit flip)	$\begin{pmatrix} 0 & 1 \\ 1 & 0 \end{pmatrix}$	
Pauli Z (phase flip)	$\begin{pmatrix} 1 & 0 \\ 0 & -1 \end{pmatrix}$	
Hadamard	$\frac{1}{\sqrt{2}} \begin{pmatrix} 1 & 1 \\ 1 & -1 \end{pmatrix}$	
CNOT (CX)	$\begin{pmatrix} 1 & 0 & 0 & 0 \\ 0 & 1 & 0 & 0 \\ 0 & 0 & 0 & 1 \\ 0 & 0 & 1 & 0 \end{pmatrix} \begin{pmatrix} 1 & 0 & 0 & 0 \\ 0 & 0 & 0 & 1 \\ 0 & 0 & 1 & 0 \\ 0 & 1 & 0 & 0 \end{pmatrix}$	
Toffoli (CCNOT)	$\begin{pmatrix} 1 & 0 & 0 & 0 & 0 & 0 & 0 & 0 \\ 0 & 1 & 0 & 0 & 0 & 0 & 0 & 0 \\ 0 & 0 & 1 & 0 & 0 & 0 & 0 & 0 \\ 0 & 0 & 0 & 1 & 0 & 0 & 0 & 0 \\ 0 & 0 & 0 & 0 & 1 & 0 & 0 & 0 \\ 0 & 0 & 0 & 0 & 0 & 1 & 0 & 0 \\ 0 & 0 & 0 & 0 & 0 & 0 & 0 & 1 \\ 0 & 0 & 0 & 0 & 0 & 0 & 1 & 0 \end{pmatrix}$	

Finally, a measurement is applied to the end of the circuit in order to output the final state of the system. Since this breaks any superposition and entanglement within the system, it is an irreversible operation, and therefore not a quantum gate. It projects the state to one of the basis vectors, since they were designed to be eigenstates, with the probability of it landing in any one basis simply being the square of that vector's length - as you would expect from a quantum mechanical system. This is represented on a quantum circuit as ⟨measurement symbol⟩.

5.3.4 Quantum gates using braiding

The gates that have been introduced are incredibly powerful, as has been shown by the many theories outlined in the introduction. However, to implement such a tool, we need a quantum system to create such a computational device. As we know, the braiding of anyons requires the use of unitary matrices called F-matrices and R-matrices, and since

quantum gates are all necessarily defined using unitary matrices, we postulate that though a series of braids, it is possible to build quantum gates and, hence, build a topological quantum computer.

In order to perform any computations we first need to produce our topological qubits from the vacuum. This is achieved through two pair productions, creating four Fibonacci anyons with a total 'charge' of 0, meaning they must also fuse to the trivial anyon **0** since they were created from the vacuum. This can be done through two fusion routes: '**0**τ**0**' and '$\tau\tau$**0**'. Since our first qubit pair fuse either a **0** or τ, we will label those states as a $|0\rangle$ and $|1\rangle$, respectively. Because the four anyons have a net charge of 0, the braiding of the first and second anyon is identical to braiding the third and fourth anyon, making the second braid irrelevant and redundant. Therefore, it is possible to compute all gate operations through the braiding of just three anyons in our gate, with the fourth anyon simply used to initialise the system. [35]

Therefore, all gates which affect only one anyon, like the Hadamard gate and the NOT gate, should only consist of a weave with one warp anyon and two weft anyons. We have seen an example of such as weave when looking at the injection weave in Fig. 22. To find a series of braids which replicate the desired operation with a satisfactory level of precision is simply a method of brute force and exhaustive trial and error [38]. Fortunately, some of the properties of Fibonacci anyons narrow down the possible braids

- six consecutive identical braids is equivalent to four inverse braids, therefore any braid network with six consecutive identical braids can be rejected

- Due to braiding identities and the topology of our system, certain triplets are equal to others (through F and R moves)

- If a braid and it's inverse braid are consecutive, this is simply the identity so the braid can be rejected

Using these equivalencies, a set of 18 braids, for example, can be reduced from 91,625,968,980 combinations to just 33,527,163 different options [37]. Adding braids,

48

while increasing the complexity of the operation, increases the accuracy of the gate to mimic the intended operation. Exchanging the braids for a weave network will also increase the length of network since injection weaves are required in order to move the warp anyon across the different weft anyons. However this significantly reduces the practical complexity of implementing such a system. Below are the weaves that have been found the represent popular quantum gates as well as an error margin of the gate.

Figure 23: A weave which approximates to the Hadamard gate [37]

Fig. 23 shows a weave which approximates to the Hadamard gate with an error of 0.0003. The braid consists of 24 braiding operations and leads to the matrix [37]

$$e^{3.4558i}\frac{1}{\sqrt{2}}\begin{pmatrix} 0.9997 + 0.0017i & 1.0003 - 0.0039i \\ 1.0003 + 0.0039i & -0.9997 + 0.00017i \end{pmatrix}. \tag{46}$$
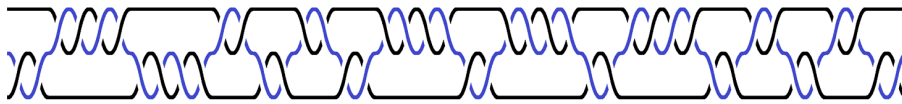

Figure 24: A weave which approximates to the Pauli X (NOT) gate [37]

Fig. 24 shows a weave which approximates to the NOT gate with an error of 0.00086. The braid consists of 44 braiding operations.

Figure 25: A weave which approximates to the phase gate [37]

Fig. 25 shows a weave which approximates to the phase gate with an error of 0.0045. The braid consists of 36 braiding operations

Since the CNOT gate requires a target qubit and a control qubit, the braid requires the presence of two qubits, each represented by three anyons. Each qubit has it's own
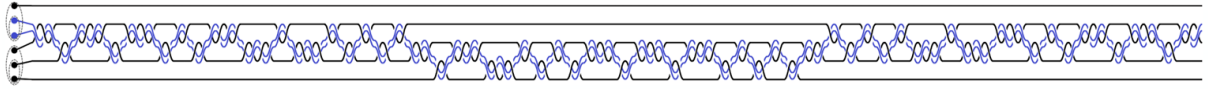
Figure 26: A braid which approximates to the CNOT gate [37]

warp anyon (in blue) however they both braid with the same anyon across the entire particle. This gate has an error of 0.0007 while requiring 280 separate braiding operations. However, the theorem explored earlier tells us that any braid can be represented by a weave, applying this provides a more efficient method of carrying out the quantum computation with only 1 warp anyon. Fig. 27, is the weave that carries out the same operation as the braid in Fig. 26 with an error of 0.0032. Therefore, while the weave is more practical and clearly requires less gates, it comes at the cost of accuracy.
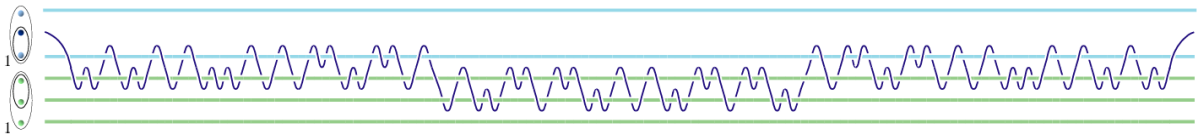

Figure 27: A weave which approximates to the CNOT gate [38]

An example of gates coming together to perform an algorithm can be see in Fig. 28. This is the braid common in an AJL alogorithm and is used to calculate the Kauffman invariant of a knot [37]. As described earlier, calculating the Kauffman invariant of a knot is an exponentially difficult problem, however by constructing a knot using a quantum computer, this problem can be simplified down to a polynomial time problem. The AJL algorithm is one such method of doing so. From the matrix representation of the Hadamard gate above, we can see that the weave approximations of gates often pick up a general phase. To remove this arbitrary phase, a phase gate can be applied at the end of the computation in order to correct any algorithms to output the expected result. [37]

From this review, we can see that it is possible to build quantum gates that can perform the same computations as a classical computer in a much faster time. It is possible to build these gates through the braiding of quasiparticles formed in a two-dimensional fractional quantum Hall state due to a magnetic field applied perpendicular to the plane. Building gates to a high accuracy requires a lot of separate braids and
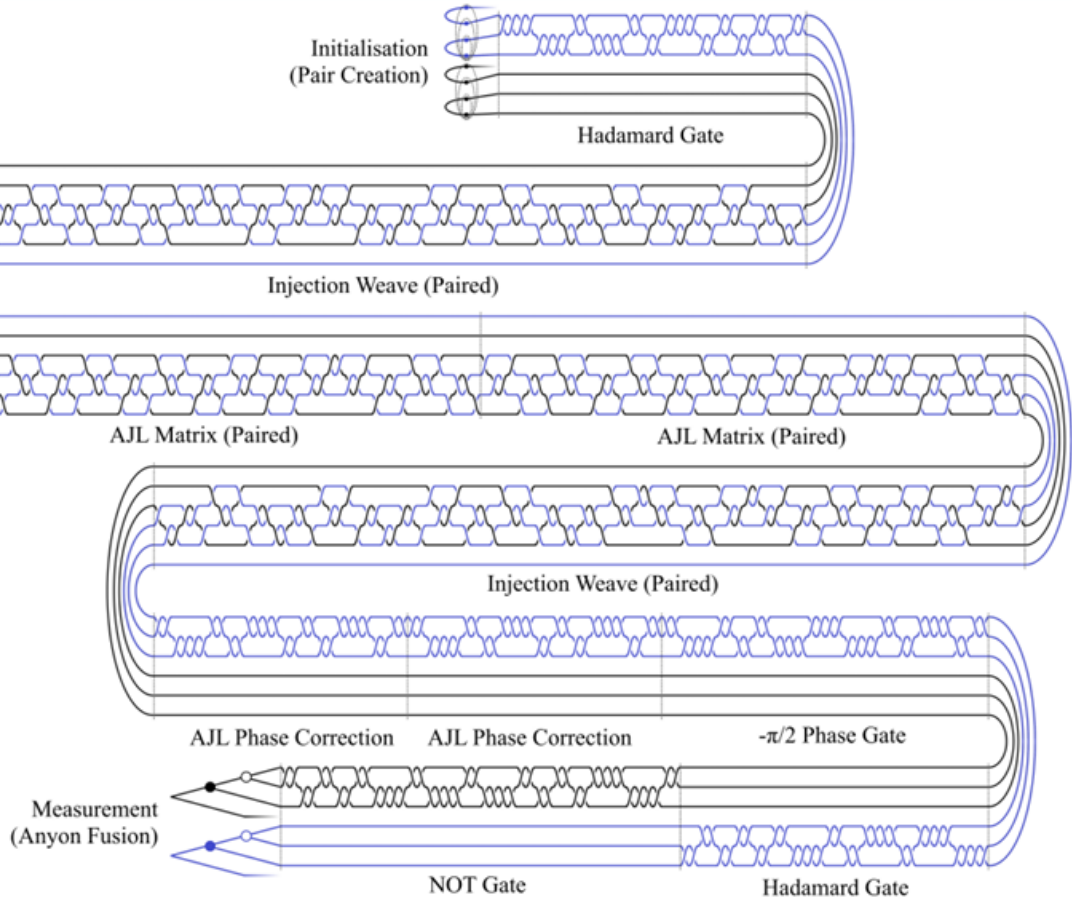
Figure 28: A typical braid used to compute the AJL algorithm [37]

complete algorithms can require the use of millions of separate braiding actions. For example, evaluating the trace closure in the AJL algorithm requires 93,437,024 separate individual braids [37]. In order to make this process easier, it is possible to complete all braids by moving only one warp anyons while holding all other anyons in a fixed position. The output of any quantum algorithm is achieved by measuring the state, collapsing the superposition, which is done by fusing all the anyons back together and observing the final result. The final part to consider is how a topological quantum computer can experience errors and what processes can be used to prevent such errors from occurring.

6 Errors

In non-topological quantum computing arise in two different ways: 1. Errors from the imprecision of quantum gates when approximated by a series of braids 2. Decoherence of a system which affects the superposition of the qubit. Both of these errors can be quantified using either fidelity distance or a super-operator norm [40]. These errors must be rectified using error-correction codes such as the Shor's algorithm or the toric code, or must be averted using a fault-tolerant quantum computer. These techniques may be used to create an error tolerant quantum computer as long as the probability for an error is under a certain threshold - known as the 'threshold theorem for quantum computation'. This theorem asserts that an arbitrarily long quantum computation can be conducted reliably provided the quantum noise of the system is lower than the threshold ε_{th} [39]. Most papers put this value to be between the ranges of 10^{-5} and 10^{-3}, with the more optimistic values for higher fault tolerance from the system itself [40].

However, instead of attacking the problem of lowering the accuracy threshold head on, topological quantum computing provides an immunity from any local errors creating an error in the system. By creating topological qubits which are simply degenerate ground states of a given system, only global operations which change the ground state can effect the ground state and any local changes does not change the state of the qubit. Fig. 12 shows how a small perturbation to the world line doesn't effect ground state since the Kauffman invariant of such a knot would still remain - therefore the amplitude of the system wouldn't change when $\langle GS_a|GS_b\rangle$ is calculated using the Kauffman polynomial method.[34]

The only way that errors can occur in a topological quantum computer is if the error is non-local and interferes with the ground state of the topological system. However, there is usually an easy fix to prevent a global error from occurring. An example of such an error would be a scenario where spontaneous pair production occurs, one anyon braids around an anyon belonging to a qubit in such a way that it disturbs the ground state of

the system, and then fuses with the anyon it was produced with. Ising anyons of the $\frac{5}{2}$ filling fraction are an example of a non-Abelian anyon which would remain completely unaffected by such a braiding, although Ising anyons are harder to build a topological quantum computer around. [31]

Another example of errors in topological quantum computing can be seen in the toric code, which uses a combination of Plaquette operators and Vertex operators to construct a very similar model to what we have produced. However, the computation takes place on a lattice on a torus manifold. On the lattice of the torus manifold, errors can be produced when random points on the lattice are flipped again and again until there is an entire loop on the torus that has been created through these errors. This changes to parity of the system along a handle of the torus, changing the ground state of the system. This can be fixed simply by increasing the size of the torus such that the chance of so many errors occurring in that manner is close to nil. [31]

This all goes to show that topological quantum computing is a robust fault-tolerant method of quantum computing which sidesteps the problem of decoherence in a quantum system simply by creating a global qubit using the principles of knot theory. Instead, the only errors that remain in the the topological model are the approximations of gates when using a weave to simulate the desired output. However, our system doesn't try to measure the state of the quantum system while it is in a superposition, but instead measures the ground state after all final fusion has occurred during measurement. Therefore, a subtle change in probability of any one anyon fusing with another has little to no effect on the final outcome of the system, making errors incredibly rare.

7   Conclusion

As classical computing reaches its limiting factor of size and its ability to conduct powerful operation, humanity must turn to a new method of computing in order to technologically progress in the same way it has been for the past century. On paper, quantum computing seems to be the solution to all its problems. However, when considering the environments in which physical systems can maintain a quantum coherence, we observe that these conditions are vastly different to those of everyday life.

Due to this, the realisation of quantum computing has been a very difficult task for physicists and engineers since the turn of the century. To maintain coherence of most non-topological quantum states, the system must be cooled to very low temperatures and kept in a very isolated environment to prevent to collapse of the superposition of qubits.

On the other hand, we have shown in this literature review that through the use of the fractional Hall effect, we can create quasiparticles called anyons - particles which are neither fermions nor bosons but can take *any* phase. Specific classes of these anyons called Fibonacci anyons can be manipulated through a series of unitary operations called F-moves and R-moves through which quantum gates can be built. Using these operations, it is possible to build a physical model representing the braiding of anyons with each other. The braiding of anyons transforms the degenerate ground states from one to the other and the amplitudes of any transition between two ground states can be calculated through the mathematical models of knot theory called the Kauffman invariant. Every transition between different ground states is a unique transformation since they all produce a different knot meaning they have a unique knot invariant suggesting that braiding can be used to create reversible quantum gates.

The method of braiding protects the state of the system by negating the effects of any local perturbations, meaning that only global transformations can effect the system - a clear advantage when trying to build a quantum computer. By pulling anyons from the vacuum and keeping them in fixed position a reasonable distance apart, we have studied

how one anyons can be used to weave in between all other anyons in order to simulate braids to high enough levels of accuracy in order to build quantum gates.

The realisation of topological quantum computing is on the edge of innovation as physicists and engineers all over the world work to observe non-Abelian anyons and braid them. The production of physical non-Abelian anyons so far has proved difficult despite Abelian anyons being discovered and manipulated in two experiments as Purdue University. [41]

The creation of non-Abelian anyons using electrons to create vortices in two dimensional space has not been achieved yet despite multiple papers in the past being published - claiming they have. These papers have, unfortunately, been rescinded since. However, this year, two companies have used superconducting quantum processors to generalise stabiliser code and create Ising anyons. Using these, we have been able to verify the non-Abelian exchange statistics of these particles as well as their fusion rules. [42] [43]

There is debate among scientists whether these particles should be considered physical or simply simulations on a quantum processor since they are built on the structure of a toric code using regular qubits - implying they are only as error free as the non-topological qubits they are built out of [44]. That said, I believe that they are still a powerful tool to explore this novel field in any way possible. Any insight we can gain about these particles and their properties will only serve us well when solid state non-Abelian anyons are eventually realized. This literature review has shown that using Fibonacci anyons is an incredibly powerful method of producing quantum machinery that may one day find itself on everyone's desk in the future.

8 Bibliography

References

[1] https://www.etymonline.com/word/computer

[2] *Elliot K, Knight A, Cowley C.* Oxford Dictionary and Thesaurus III. 2001. Oxford University Press.

[3] *Weik M. H.* The ENIAC story. 1961. Ordnance. **45**. 244. (pp. 571-575)

[4] *Deutsche D, Jozsa R.* Rapid solution of problems by quantum computation. 1992. Proc. R. Sond. Lond. A. **439**. 1907. (pp. 553-558)

[5] *Nield D.* Google Quantum Computer Is '47 Years' Faster Than #1 Supercomputer. 2023. Science Alert.

[6] *Shor P. W.* Polynomial-Time Algorithms for Prime Factorization and Discrete Logarithms on a Quantum Computer. 1997. SIAM Review. **41**. 2. (pp. 303-332)

[7] *Stoudenmire E. M, Waintal X.* Grover's Algorithm Offers No Quantum Advantage.

[8] *Kane B. E.* A silicon-based nuclear spin quantum computer. 1998. Nature. **393**. 6681. (pp. 133-137)

[9] *Knill E, Laflamme R, Milburn G.J.* A scheme for efficient quantum computation with linear optics. 2001. Nature. **409**. 6816. (pp. 46-52)

[10] *Cirac J. I, Zoller P.* Quantum computations with cold trapped ions. 1995. Physical Review Letters. **74**. 20. (pp. 4091)

[11] *Bose S. N.* Plancks Gesetz und Lichtquantenhypothese. 1924. Zeitschrift für Physik. **26**. (pp. 178-181)

[12] *Bose S. N.* Planck's law and the light quantum hypothesis. 1994. Journal of Astrophysics and Astronomy **15** (pp. 3-11)

[13] *Travasset P. M.* Origin and foundations of Bose-Einstein statistical mechanics. 2018. diposit.ub.edu

[14] *Rajantie A.* Unification Lecture Notes. 2022.

[15] *Dirac P.* On the theory of quantum mechanics. 1926. Royal Society. **112**. 762. (pp. 661-677)

[16] *Fermi E.* Sulla quantizzazione del gas perfetto monoatomico. 1926. Rendiconti Lincei. **3**. (pp. 145-149)

[17] *Majorana E.* Teoria simmetrica dell'elettrone e del positrone. 1937. Il Nuevo Cimento. **14**. 4. (pp. 171-184)

[18] *Landau L. D.* On the Theory of the Fermi Liquid. 1959. Soviet Physics JETP. **35**. 8. (pp. 70-74)

[19] *Hall E. H.* On a new action of the magnet of electric currents. 1879. American Journal of Mathematics **2**. 3. (pp. 287-292)

[20] *Klitzing K. V, Dorda G, Pepper M.* New Method for High-Accuracy Determination of the Fine Structure Constant Based on Quantised Hall Resistance. 1980. Physical Review Letters. **45**. 6. (pp. 494-497)

[21] *Laughlin R. B.* Quantized Hall conductivity in two dimensions. 1981. Physical Review B. **23**. 10 (pp. 5632-5633)

[22] *Stormer H. L, Tsui D. C, Gossard A. C.* The fractional quantum Hall effect. 1999. Reviews of Modern Physics. **71**. 2. (pp.298-305)

[23] *Willet R et al.* Observation of an Even-Denominator Quantum Number in the Fractional Quantum Hall Effect. 1987. Physical Review Letters. **59**. 15. (pp. 1776-1779)

[24] *Wilczek F.* Anyons. 1991. Scientific American. **264**. 5. (pp. 58-65)

[25] *Wilczek F.* Quantum Mechanics of Fractional-Spin Particles. 1982. Physical Review Letters. **49**. 14. (pp. 957-959)

[26] *Wilczek F.* Magnetic Flux, Angular Momentum, and Statistics. 1982. Physical Review Letters. **48**. 17. (pp. 1144-1146)

[27] *Rao S.* Introduction to abelian and non-abelian anyons. 2016. arxiv ePrint 1610.09260

[28] *Mani H. S. et al.* Topology and Condensed Matter Physics. 2017. Hindustan Book Agency. **19**.

[29] *Trebst S, Troyer M, Wang Z, Ludwig A. W. W.* A short introduction to Fibonacci anyon models. 2008. Oxford University Press. **176** (pp. 384-407)

[30] *Corwell R. H, Fox R. H.* Introduction to Knot Theory. 1963. Springer-Verlag

[31] *Simon S. H.* Topological Quantum Computing. CSSQI. 2012. University of Waterloo

[32] *Reidemeister K.* Knot Theory. 1983. BCS Associates.

[33] *Kauffman L. H.* Knots and Physics. 2001. World Scientific Publishing. **3**

[34] *Witten E.* Quantum Theory and the Jones Polynomial. 1989. Communications in Mathematical Physics. **121** (pp.351-399)

[35] *Nayak C. et al.* Non-Abelian Anyons and Topological Quantum Computation. 2008. Reviews of Modern Physics. **80**. 3. (pp. 1083-1156)

[36] *Simon S. H. et al* Topological Quantum Computing with Only One Mobile Quasiparticle. 2006. Physical Review Letters. **97**. 7.

[37] *Field B, Simula T.* Introduction to topological quantum computation with non-Abelian anyons. 2018. Quantum Science and Technology. **3**.

[38] *Hormozi L, Zikos G, Bonesteel N. E, Simon S. H.* Topological Quantum Compiling. 2007. Physical Review B. **75**. 16. arXiv preprint quant-ph/0703264.

[39] *Aliferis P, Gottesman D, Preskill J.* Accuracy Threshold for Postselected Quantum Computation. 2007.

[40] *Freedman M. H, Kitaev A, Larsen M. J, Wang Z.* Topological Quantum Computation. 2002. American Mathematical Society. **40**. 1. (pp.31-38)

[41] Nakamura J, Liang S, Gardner G. C, Manfra M. J. Impact of bulk-edge coupling on observation of anyonic braiding statistics in quantum Hall interferometers. 2022. Nature Communications. **13**. 344.

[42] *Anderson T. I. et al.* Non-Abelian braiding of graph vertices in a superconducting processor. 2023. Nature. pp(1-6)

[43] *Iqbal M.* Creation of Non-Abelian Topological Order and Anyons on a Trapped-Ion Processor. 2023. arXiv preprint arXiv:2305.03766.

[44] *Wood C.* Physicists Create Elusive Particles That Remember Their Pasts. 9th May 2023. Quanta Magazine.

[45] *Sumners D. W.* The knot theory of molecules. 1987. Journal of Mathematical Chemistry. **1**. (pp. 1-14)